NPS-63-87-008

NAVAL POSTGRADUATE SCHOOL

Monterey, California

CORRECTION OF THE WIND FIELD MEASURED BY THE NCAR ELECTRA DURING FASINEX FOR INERTIAL NAVIGATION SYSTEM DRIFTS

WILLIAM J. SHAW

GAIL T. VAUCHER

OCTOBER 1987

FASINEX Contribution No. 18

Prepared for: National Science Foundation
Washington, DC 20550

NAVAL POSTGRADUATE SCHOOL
Monterey, California

Rear Admiral R. Austin
Superintendent

K. Marshall
Provost (Acting)

The work reported herein was supported in part by the National Science Foundation (Ocean Sciences) with funds provided by Grant OCE-86-03050.

This report was prepared by:

REPORT DOCUMENTATION PAGE

1a REPORT SECURITY CLASSIFICATION: Unclassified	1b RESTRICTIVE MARKINGS
2a SECURITY CLASSIFICATION AUTHORITY	3 DISTRIBUTION/AVAILABILITY OF REPORT: Approved for public release; distribution unlimited
2b DECLASSIFICATION/DOWNGRADING SCHEDULE	
4 PERFORMING ORGANIZATION REPORT NUMBER(S): NPS-63-87-008	5 MONITORING ORGANIZATION REPORT NUMBER(S)
6a NAME OF PERFORMING ORGANIZATION: Naval Postgraduate School; 6b OFFICE SYMBOL (If applicable): 63	7a NAME OF MONITORING ORGANIZATION
6c ADDRESS (City, State, and ZIP Code): Monterey, CA 93943-5000	7b ADDRESS (City, State, and ZIP Code)
8a NAME OF FUNDING/SPONSORING ORGANIZATION: National Science Foundation; 8b OFFICE SYMBOL (If applicable)	9 PROCUREMENT INSTRUMENT IDENTIFICATION NUMBER: NSF Grant OCE-86-03050
8c ADDRESS (City, State and ZIP Code): Washington, DC 20550	10 SOURCE OF FUNDING NUMBERS: PROGRAM ELEMENT NO; PROJECT NO; TASK NO; WORK UNIT ACCESSION NO

11 TITLE (Include Security Classification)
Correction of the Wind Field Measured by the NCAR Electra During FASINEX for Inertial Navigation System Drifts

12 PERSONAL AUTHOR(S)
William J. Shaw and Gail T. Vaucher

13a TYPE OF REPORT	13b TIME COVERED	14 DATE OF REPORT (Year, Month Day)	15 PAGE COUNT
Technical	FROM 11/86 TO 12/88	October 1987	43

16 SUPPLEMENTARY NOTATION

17 COSATI CODES		
FIELD	GROUP	SUB-GROUP

18 SUBJECT TERMS (Continue on reverse if necessary and identify by block number)
FASINEX
Aircraft Meteorological Measurements
Atmospheric Boundary Layer

19 ABSTRACT (Continue on reverse if necessary and identify by block number)

This report describes a technique for removal of inertial navigation system drifts from winds measured by the NCAR Electra during the Frontal Air-Sea Interaction Experiment (FASINEX) in 1986. Without correction, horizontal wind divergences calculated from these data may contain errors as large as 10^{-4} s^{-1} resulting from the Schuler oscillation. After correction, the divergence error is reduced by at least an order of magnitude. Correction coefficients and a subroutine to use them were provided for the five of six FASINEX flights for which correction was possible.

20 DISTRIBUTION/AVAILABILITY OF ABSTRACT	21 ABSTRACT SECURITY CLASSIFICATION	
☒ UNCLASSIFIED/UNLIMITED ☒ SAME AS RPT ☐ DTIC USERS	Unclassified	
22a NAME OF RESPONSIBLE INDIVIDUAL: William J. Shaw	22b TELEPHONE (Include Area Code): (408) 646-3430	22c OFFICE SYMBOL: 63Sr

DD FORM 1473, 84 MAR 83 APR edition may be used until exhausted
All other editions are obsolete

TABLE OF CONTENTS

ABSTRACT

This report describes a technique for removal of inertial navigation system drifts from winds measured by the NCAR Electra during the Frontal Air-Sea Interaction Experiment (FASINEX) in 1986. Without correction, horizontal wind divergences calculated from these data may contain errors as large as 10^{-4} s^{-1} resulting from the Schuler oscillation. After correction, the divergence error is reduced by at least an order of magnitude. Correction coefficients and a subroutine to use them were provided for the five of six FASINEX flights for which correction was possible.

1. INTRODUCTION: THE FASINEX FIELD PROGRAM

1.1 Role of the NCAR Electra

The Frontal Air-Sea Interaction Experiment (FASINEX) is a field measurement program which occurred January through March of 1986 in the Sargasso Sea. The objectives and experimental plan for this project have been explained in detail by Stage and Weller (1985,1986). In general, the purpose of the work was to investigate the structure of and the interactions between the oceanic and marine atmospheric boundary layers in the presence of the relatively simple inhomogeneity of a subtropical ocean front. Investigators from the University of California (Irvine), the National Center for Atmospheric Research (NCAR), and the Naval Postgraduate School (NPS) participated in this effort using the Electra aircraft operated by NCAR. The Electra's primary use was for the measurement of the horizontal variation of mean atmospheric variables and turbulence fluxes in the atmospheric surface layer. To accomplish this, the Electra flew a pattern of overlapping boxes at an altitude of approximately 35 m as described by Stage and Weller (1986).

1.2 Need for Accuracy in Aircraft Winds

The mean and slowly varying behavior of the horizontal wind field is of particular importance to the FASINEX analysis. The cross-isobaric angle of the momentum budget and the advection terms of that budget (and other budgets as well) require that the mean wind be determined with the greatest possible accuracy. It is expected that the horizontal momentum flux and stability variations resulting from sea-surface temperature changes across the ocean front will also induce secondary circulations in the ABL. These secondary circulations should be evident in the surface divergence and vorticity fields, which we intend to obtain from the aircraft wind measurements.

Divergence and vorticity measurements may be obtained from aircraft by line integral calculations or by differentiating surfaces fit to the horizontal velocity fields. For either method, rather accurate winds are required. Lenschow and Spyers-Duran (1987) have considered the uncertainty which a velocity error growing linearly with time would cause in line integral calculations of these two quantities. As subsequent sections will show, it is more realistic to consider sinusoidally varying wind component errors with periods of slightly greater than 84 min.

2. PROCESS OF AIRCRAFT WIND MEASUREMENT

2.1 General Method

The measurement of the wind velocity from an aircraft is a vector subtraction process in which the aircraft motion relative to the atmosphere is subtracted from the aircraft motion relative to the earth's surface. The difference is then the desired air motion vector. Lenschow and Spyers-Duran (1987) describe in detail the methods by which these measurements are made aboard the NCAR Electra. Basically, the aircraft motion relative to the air is sensed by a gust probe system which consists of fixed vanes and a pitot-static probe mounted on a boom 5 m in front of the aircraft. Aircraft motion relative to the earth's surface is determined by integrations of the output from a Schuler-tuned accelerometer. (The Electra uses the LTN-51 by Litton Systems, Inc.) This will be discussed further in section 3.1.

2.2 Sources of Error in Aircraft Winds

2.2.1 Gust probe errors

Each of the motion measurement systems on the aircraft is subject to error. The gust probe measurements are susceptible to biases in the measurement of the airspeed vector due to upwash effects around the gust probe. Since it is not feasible to calculate these biases based upon ground-based measurements, the Electra is put through the "Lenschow maneuvers" on each flight day (Lenschow and Spyers-Duran). During these maneuvers, which are commonly done on the ferry home, the aircraft attitude is varied over large pitch and yaw angles. Additionally, the airspeed is varied through speed runs from near-stall to maximum cruising speeds. Other biases may be removed by short reverse-heading runs under the assumption that the wind velocity field remains constant. For cases in which reverse-heading runs are not performed, Grossman (1977) has outlined a method which takes advantage of ordinary flight geometry to accomplish the same purpose.

Another source of potential gust probe error in the calculation of airspeed involves the determination of specific heat at constant pressure c_p for air. Lenschow and Spyers-Duran (1987) have argued that c_p variations arising because of changes in flight level humidity can cause significant errors in the airspeed determination from the pitot-static probe. The above problems are noted but will not be discussed further in this report.

2.2.2 Inertial navigation errors

The inertial navigation system (INS) on board the Electra is essentially a gimballed set of accelerometers which measures the

accelerations experienced by the aircraft in three dimensions. These accelerations are then integrated once to obtain aircraft motion and again to obtain aircraft position. In order to cope with the relatively large acceleration due to gravity, the accelerometers are maintained in a fixed orientation relative to the local vertical. This process is accomplished by the application of appropriate torques based on position changes computed from accelerations measured during the flight and is called Schuler tuning (e.g., Broxmeyer, 1964).

It is impossible to perfectly align an INS so that its vertical coordinate is precisely parallel to the gravity vector at the beginning of a flight. As a result, a small portion of the acceleration of gravity is perceived by the INS as a horizontal acceleration, and the integrations of this error produce errors in velocity and position of the aircraft relative to the earth. The error which results from the initial misalignment of the platform is known as the Schuler oscillation and is shown by Lenschow and Spyers-Duran (1987) to have a period of 84.4 min. Accelerometer saturation (as in sharp turns) and other noise combine to give errors which unpredictably modify the phase and amplitude of the Schuler oscillation and produce other drifts as well.

3. CORRECTION OF INS WIND ERRORS

3.1 General Scheme

It is not possible to correct INS errors in aircraft data without recourse to independently determined position information. However, if an aircraft records accurate position measurements at intervals which are short compared to the Schuler period, it is possible to almost completely remove the effects of the Schuler oscillation and other inertial drifts from the horizontal wind vector.

The NCAR Electra now records position information from the Loran-C navigational aids operated by the US Coast Guard. The data, which have a specified accuracy of .25 n mi --or about 500 m--in the vicinity of the FASINEX measurement area (U. S. Coast Guard, 1980), are sampled at a rate of 1 s^{-1} and recorded as part of the standard meteorological data stream on the aircraft.

The utility of using the Loran-C information to remove inertial drifts in aircraft data has previously been demonstrated by Nicholls (1983). Nicholls applied a correction, similar to that which will be described here, to the data collected by the United Kingdom's C-130 meteorological research aircraft during the 1978 Joint Air-Sea Interaction Experiment (JASIN) in the North Atlantic. He claimed accuracies for his corrected winds of roughly 0.3 m s^{-1}.

The general approach to the correction of the aircraft winds for FASINEX is described as follows. The motion of the aircraft relative to

the earth may be expressed as the vector sum of the aircraft motion relative to the air and the air motion relative to the earth, or

$$\vec{G} = \vec{A} + \vec{V}$$

or

$$\vec{V} = \vec{G} - \vec{A}$$

where $\vec{G}$ is the aircraft ground velocity vector, $\vec{A}$ is vector aircraft motion relative to the atmosphere, and $\vec{V}$ is the net atmospheric motion.
In terms of position,

$$\vec{G}_{INS} = \frac{\partial}{\partial t}\vec{X} \qquad \text{and} \qquad \vec{G}_{TRUE} = \frac{\partial}{\partial t}\vec{X}$$

$$\vec{G}_{ERROR} = \frac{\partial}{\partial t}(\vec{X}_{INS} - \vec{X}_{TRUE}) = \frac{\partial}{\partial t}\Delta\vec{X}$$

and it follows that

$$\vec{V}_{TRUE} = \vec{V}_{INS} - \vec{G}_{ERROR}$$

The aircraft winds may thus be corrected by subtracting the ground velocity error vector from the NCAR-supplied wind vector.

3.2 Results from FASINEX

3.2.1 Position errors based on LORAN-C

The figures of Appendix A show raw position differences in km between the Electra's INS and the Loran-C receiver as a function of time for directions east and north of the 28°N, 70°W reference point (approximately the center of the Electra's FASINEX box pattern). Also shown for each flight is the aircraft track, which indicates the north-south and east-west legs of the flight pattern. These data are included to illustrate one difficulty in using Loran-C data at the edges of coverage areas. There are sharp jumps as large as 5 km occasionally and simultaneously in both components of the position differences. This effect appears to be unrelated to aircraft turns and is more than likely a result of atmospheric effects on Loran-C signal transmission. Specifically, Loran-C positions are determined by precisely measured differences in the reception time of signals from the geographically widely separated stations of a particular Loran-C chain. On the edges of a particular chain's reception area, a sky wave refracted to a particular receiver may be as strong as or even stronger than the directly transmitted ground wave. If a receiver alternately locks onto a ground wave and a sky wave, jumps such as in the plots for the flight of February 18 would result.

The removal of the jumps in position differences described above is the only subjective portion of the Electra's wind correction and was a significant requirement only for the flight of February 18. The flights of February 16, 17, 21, and 24 required very little correction, while the flight of February 20 contained so many large discontinuities that wind correction was not attempted. It is notable that weather conditions were the least disturbed of the experiment on the former days and were highly disturbed on the latter. The flight of February 20 occurred while a significant (but not forecast!) storm was over the FASINEX area. Since the atmospheric refractive index is a function of temperature and humidity (Bean and Dutton, 1966; Battan, 1973), such disturbed conditions would lead to significant variations in propagation path. Appendix A also contains the plot of the adjusted east and north position differences between the INS and the Loran-C data for February 18.

While position data were recorded at a sampling rate of 1 s^{-1}, the position data presented here are 10 s averages. The averaging was done for convenience to reduce to number of data involved in the computation of function fits described in the next sections. An obvious effect of the averaging, however, was to greatly reduce the 500 m point-to-point variability in the 1 s position difference time series (Figure 3.1). This gives reassurance in the determination of the slowly varying Schuler oscillation.

3.2.2 Velocity errors from cubic splines

As shown in section 3.1, the velocity error in each component of the INS-derived wind field is the derivative of the position error in that component. Although the 84.4-minute Schuler oscillation is obviously present in the position data, it is also apparent from the position error plots that its phase and amplitude are not constant in time. Therefore, it is not satisfactory to fit a simple sinusoid of the Schuler period to the data in order to obtain a differentiable function. We have chosen instead to use cubic splines [specifically the routine ICSICU from the International Math and Statistics Library (software product of IMSL, Houston, Texas)] . This procedure yields a function with continuous first and second derivatives.

The smoothness of the spline function depends upon the number of individual cubic segments which are joined to form the total function. Endpoints of the individual segments are termed "knots". Since endpoints are shared except at the beginning and end of the overall function, the number of knots is one more than the number of cubic polynomial segments involved in the fit. Our primary interest was resolving and removing the 84.4-min Schuler sinusoid. Since a sinusoid has two inflection points per cycle, we chose a number of knots in each fit which would yield slightly more than two inflection points in 84.4 min. This left the derivatives virtually unaffected by the higher frequency position differences, which are more likely to be caused by variations in Loran-C propagation path. Appendix B contains plots (excluding the flight of February 20) of the cubic spline functions

Figure 3.1 (a) Raw position differences (east) for February 17 with no averaging, (b) Raw position differences, but with 10 s averaging.

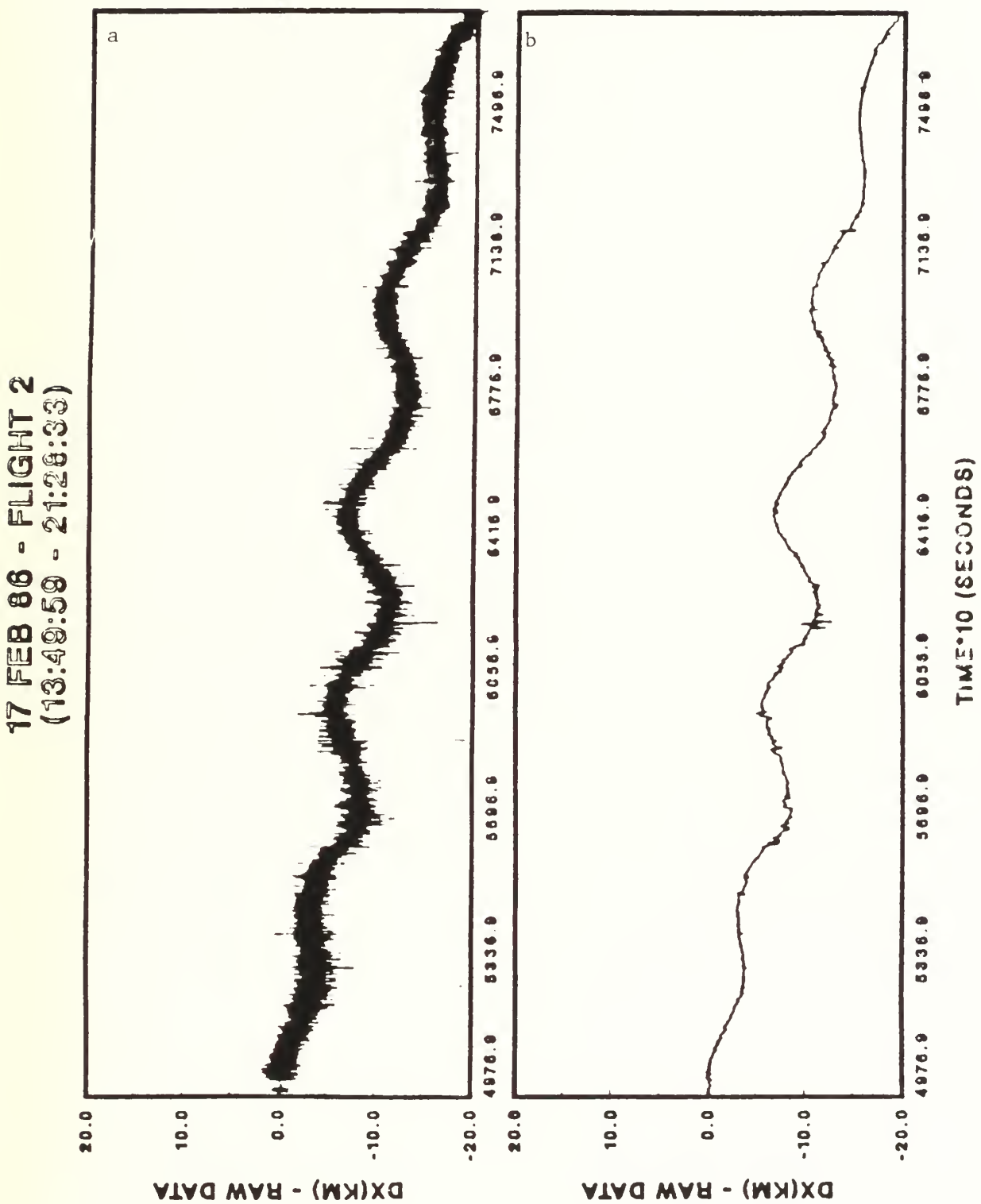

These curves are derivatives of the functions presented in Appendix B. The combination of the Schuler oscillation and a longer-term drift yield velocity errors which are typically as large as 3 m s^{-1} in each component. If one assumes a sinusoidal velocity error of this amplitude in a line integral divergence calculation using uncorrected data collected from a 100 km square box, it can be shown (Appendix F) that the error in the divergence may be as large as 1 x 10^{-4} s^{-1}. This is an order of magnitude larger than typical divergence values encountered in the undisturbed atmosphere.

It is sobering to note that because of the oscillatory nature of the position errors, there are times late in each day's flight when the position error is near zero. In the years before the Electra recorded INS-independent position information, it was common to use airport position upon landing as the single (and generally only available) external position reference for a flight. If the position error was small, the conclusion was usually that the INS drift was small and that the wind measurements, therefore, would be acceptably accurate. It is obvious from the data presented in the appendices that this is not a safe assumption.

3.2.3 Uncorrected and corrected wind fields

The figures of Appendix D show uncorrected and corrected wind vectors for the FASINEX flights (excluding February 20). These vectors are averages over 100 s intervals of the flight, which correspond to very nearly 10 km in space. Inspection of the figures shows the substantial difference the correction makes. For the flight of February 17, for example, the uncorrected winds are southeasterly with a magnitude as large as 12 m s^{-1} on the northern side of the box. On the south side, winds are nearly easterly and have a magnitude closer to 5 m s^{-1}. A vorticity calculation based on these data would result in significant cyclonic vorticity. After correction, the winds still show cyclonic vorticity, but of a smaller value. Maximum windspeeds on the north side of the box are roughly 10 m s^{-1} and minimum windspeed on the south side are closer to 7 m s^{-1}. Further, the wind vectors on the south side show much less change between the first and the second passes of the aircraft through the center of the center of that area. Uncorrected and corrected wind vector plots for the other FASINEX flights are also contained in Appendix D.

Acknowledgments: This work was performed with the support of NSF Grant OCE-86-03050. Ms. Penny Jones expertly transformed the manuscript into report form.

4. REFERENCES

Battan, L. J., 1973: Radar Observation of the Atmosphere. Chicago, University of Chicago Press, 324 pp.

Bean, B. R., and E. J. Dutton, 1966: Radio Meteorology. National Bureau of Standards Monograph 92, U. S. Department of Commerce. (Available from U. S. Government Printing Office, Washington, D. C.). 435 pp.

Broxmeyer, C., 1964: Inertial Navigation Systems. New York, McGraw-Hill, 254 pp.

Grossman, R. L., 1977: A procedure for the correction of biases in winds measured from aircraft. J. Appl. Meteor., 16, 654-658.

Lenschow, D. H., and P. Spyers-Duran, 1987: Measurement techniques: Air motion sensing. NCAR Technical Bulletin No. 23, 49 pp.

Nicholls, S., 1983: An Observational Study of the Mid-latitude, Marine Atmospheric Boundary Layer, Ph.D. dissertation, University of Southampton, U.K., 307 pp.

Stage, S. A. and R. A. Weller, 1985: The Frontal Air-Sea Interaction Experiment (FASINEX); Part I: Background and scientific objectives. Bull. Am. Meteor. Soc., 66, 1511-1520.

_____ and _____, 1986: The Frontal Air-Sea Interaction Experiment (FASINEX); Part II: Experimental plan. Bull. Am. Meteor. Soc., 67, 16-20.

U. S. Coast Guard, 1980: Loran-C User Handbook. Department of Transportation, COMDTINST M16562.3 (old CG-462), 63 pp.

A. RAW AND ADJUSTED INS--LORAN POSITION DIFFERENCES

This appendix contains plots of the position differences between the INS and the LORAN-C signal which was received by the NCAR Electra. Data are presented in an east-north geographic reference frame so that position differences are independent of flight track. Also included in each set of plots is the aircraft track versus time. Because of discontinuities the data of February 18, a plot of the adjusted data for that day immediately follows the raw data plot.

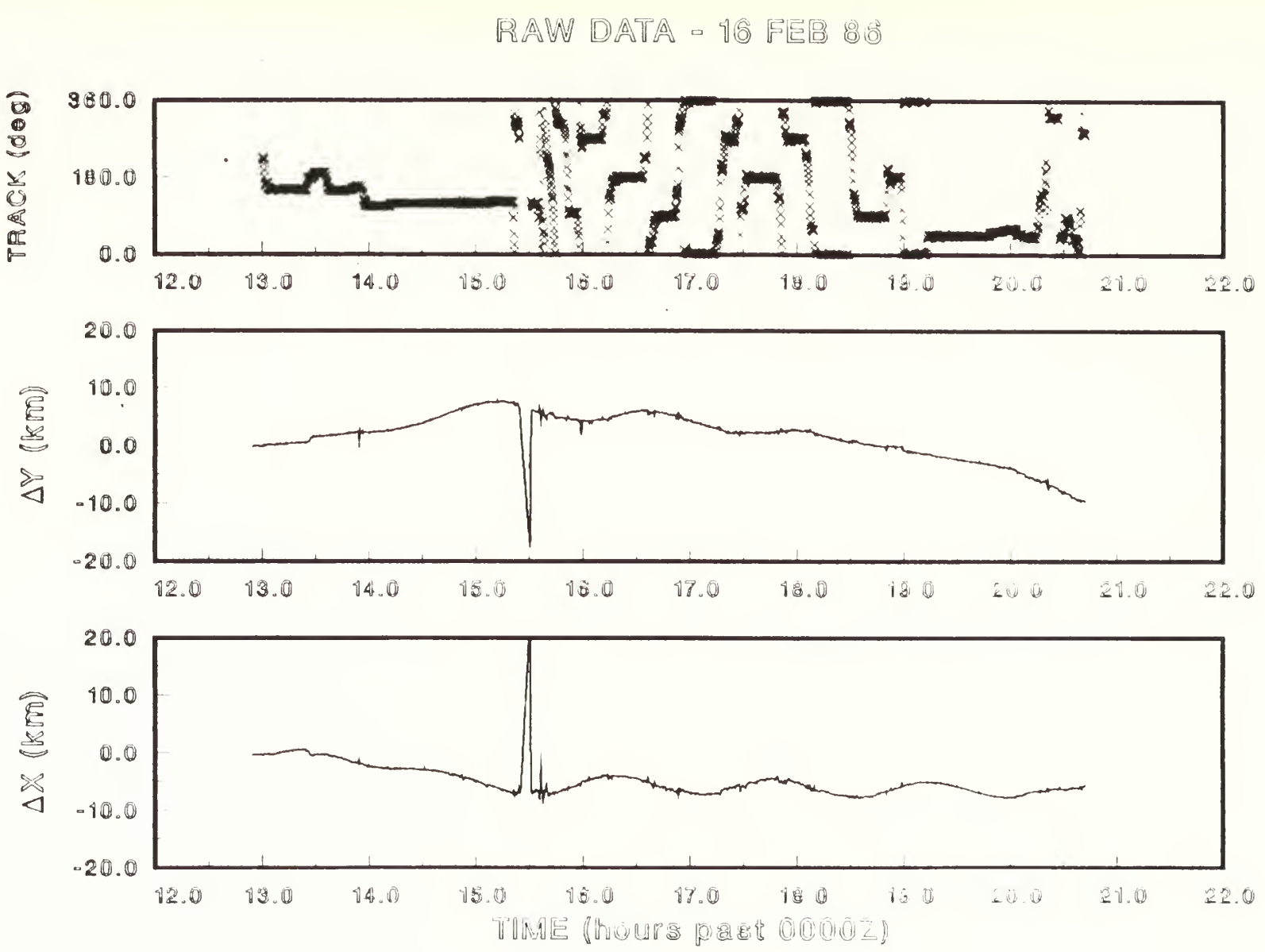
RAW DATA - 16 FEB 86
TRACK (deg)
360.0
180.0
0.0
ΔY (km)
20.0
10.0
0.0
-10.0
-20.0
ΔX (km)
20.0
10.0
0.0
-10.0
-20.0
12.0
13.0
14.0
15.0
16.0
17.0
18.0
19.0
20.0
21.0
22.0
TIME (hours past 0000Z)

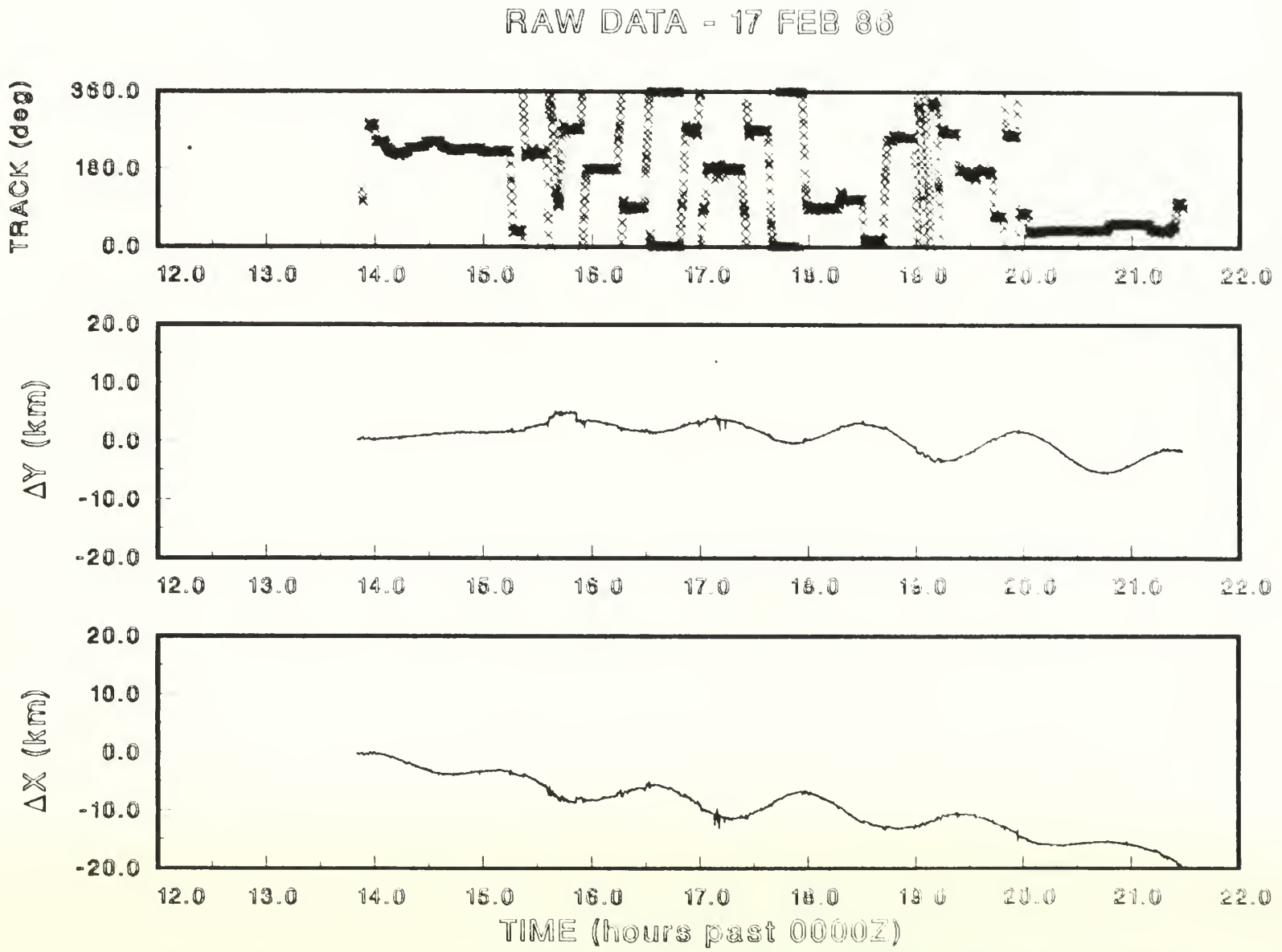
RAW DATA - 17 FEB 86
TRACK (deg)
360.0
180.0
0.0
ΔY (km)
20.0
10.0
0.0
-10.0
-20.0
ΔX (km)
20.0
10.0
0.0
-10.0
-20.0
12.0
13.0
14.0
15.0
16.0
17.0
18.0
19.0
20.0
21.0
22.0
TIME (hours past 0000Z)

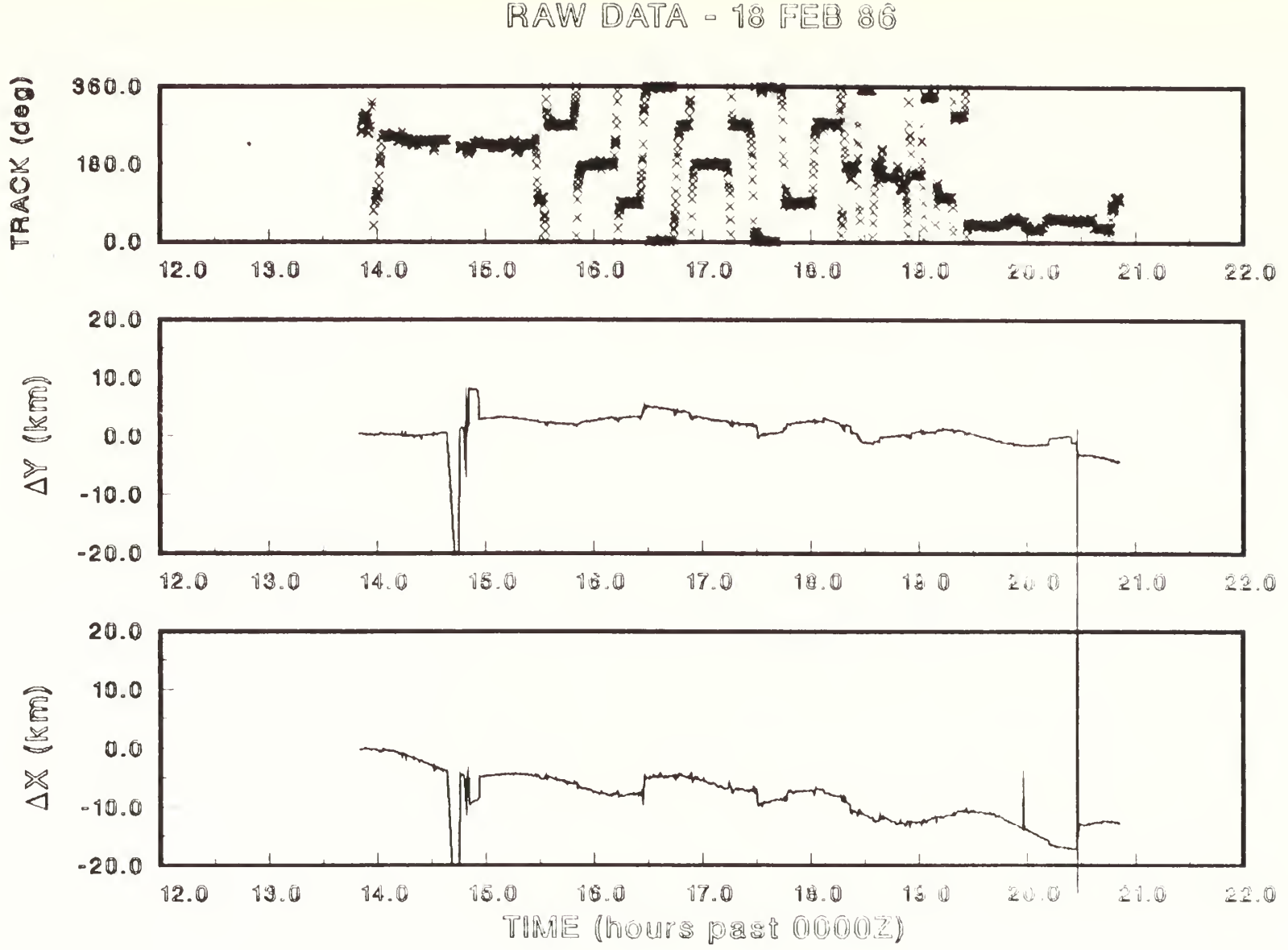
RAW DATA - 18 FEB 86
TRACK (deg)
360.0
180.0
0.0
ΔY (km)
20.0
10.0
0.0
-10.0
-20.0
ΔX (km)
20.0
10.0
0.0
-10.0
-20.0
12.0
13.0
14.0
15.0
16.0
17.0
18.0
19.0
20.0
21.0
22.0
TIME (hours past 0000Z)

CORRECTED DATA - FAS36
18 FEB 86 - FLIGHT 3

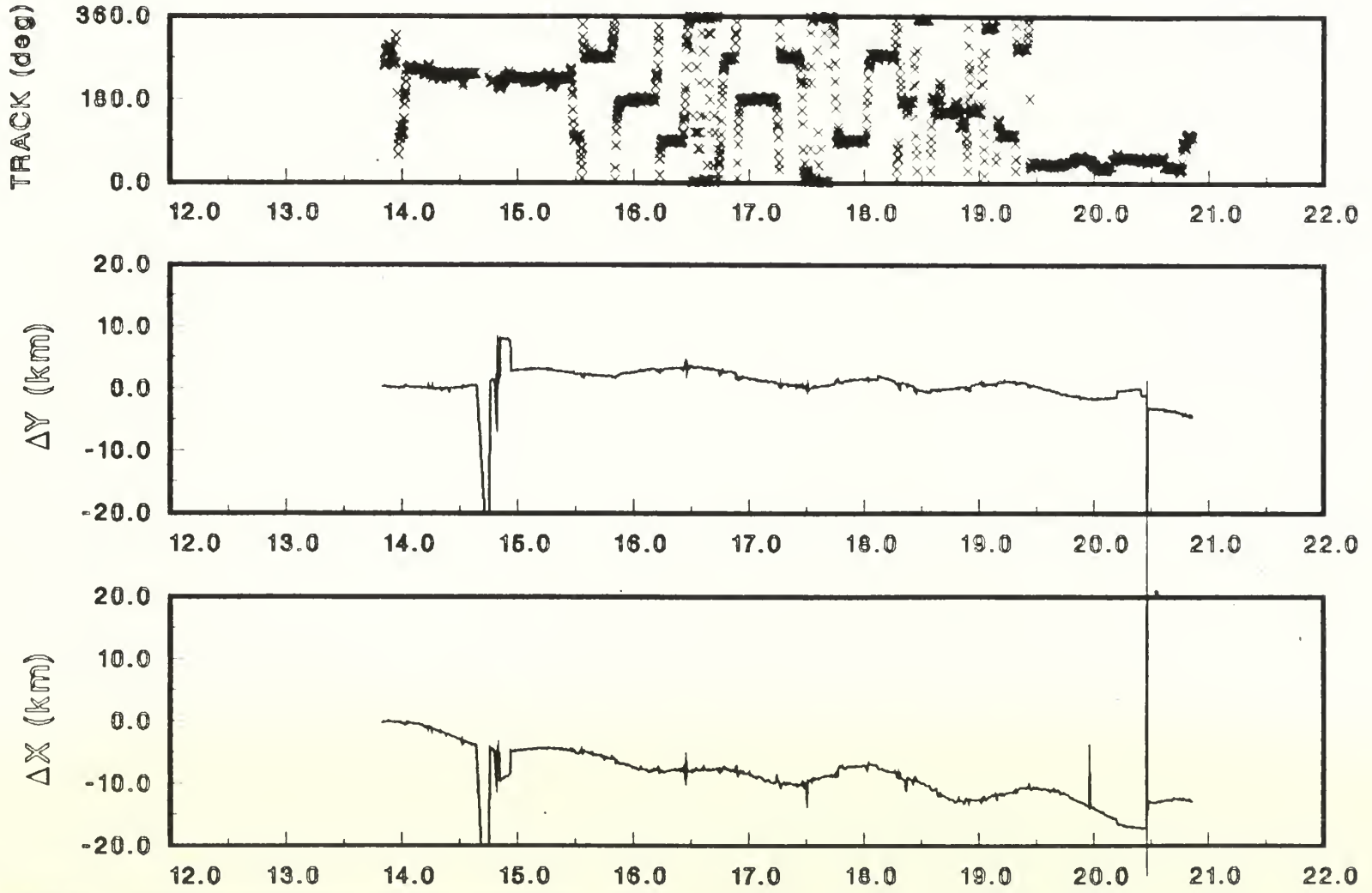

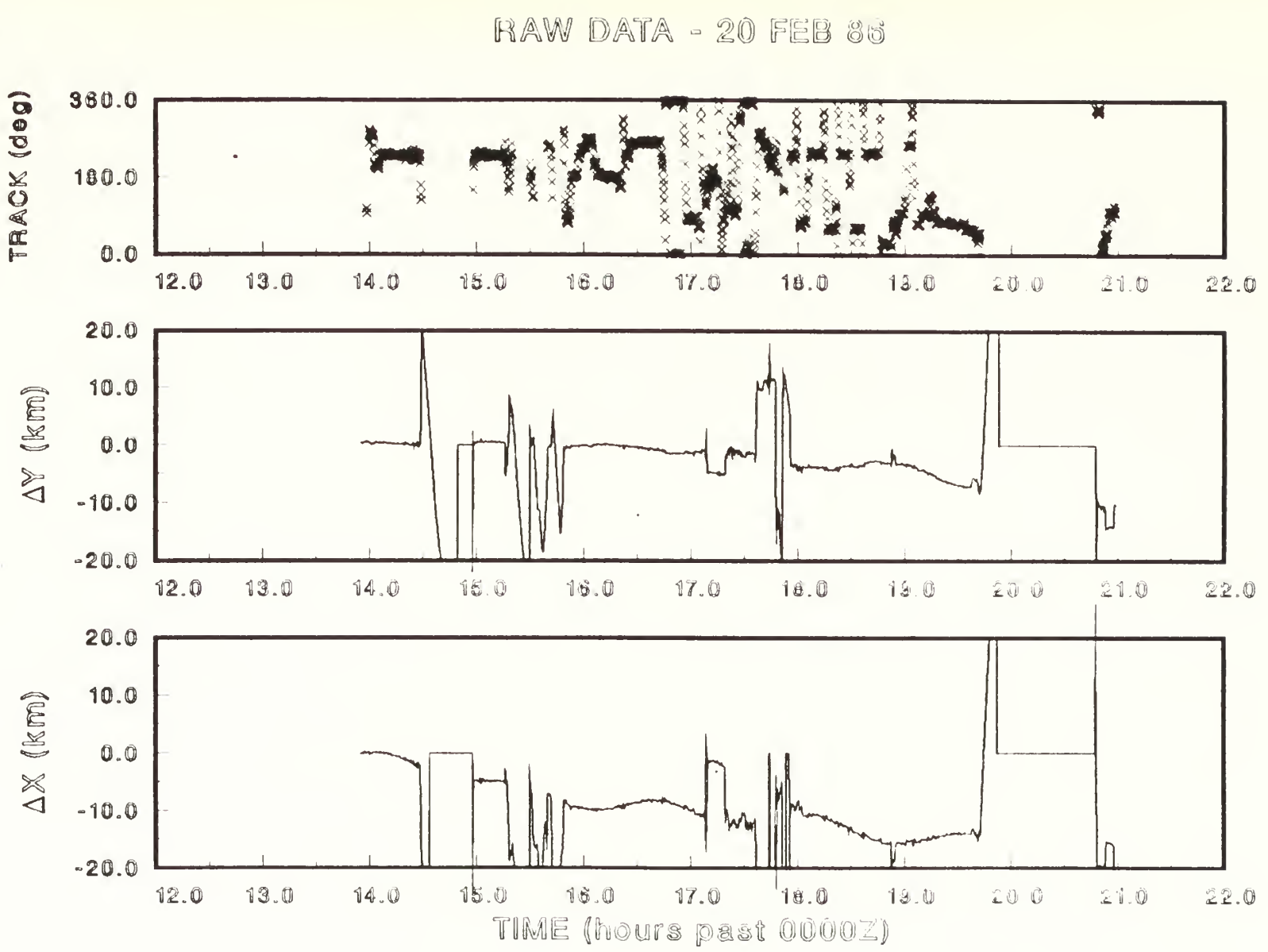
RAW DATA - 20 FEB 85
TRACK (deg)
360.0
180.0
0.0
ΔY (km)
20.0
10.0
0.0
-10.0
-20.0
ΔX (km)
20.0
10.0
0.0
-10.0
-20.0
12.0
13.0
14.0
15.0
16.0
17.0
18.0
19.0
20.0
21.0
22.0
TIME (hours past 0000Z)

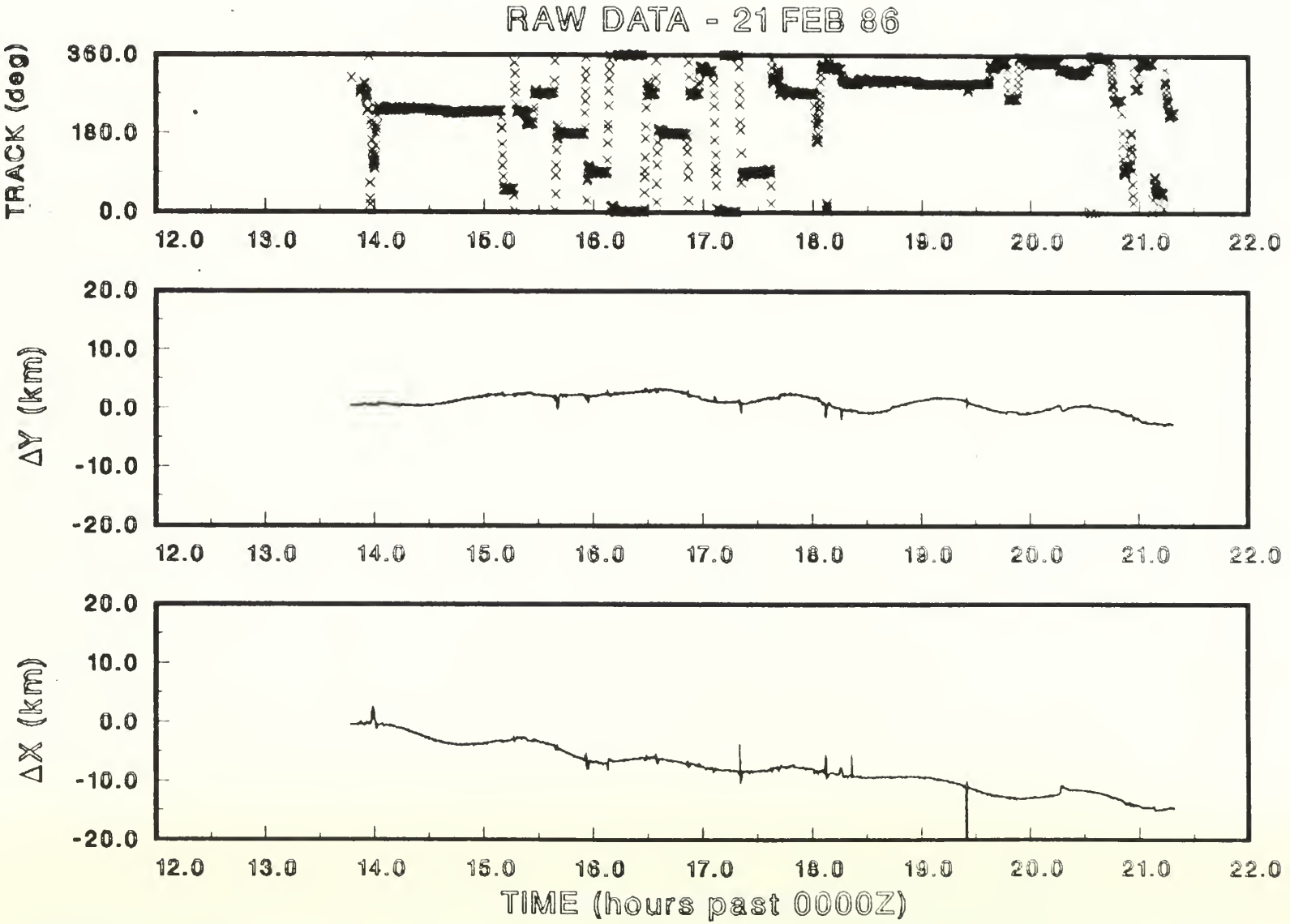
RAW DATA - 21 FEB 86
TRACK (deg)
360.0
180.0
0.0
ΔY (km)
20.0
10.0
0.0
-10.0
-20.0
ΔX (km)
20.0
10.0
0.0
-10.0
-20.0
12.0
13.0
14.0
15.0
16.0
17.0
18.0
19.0
20.0
21.0
22.0
TIME (hours past 0000Z)

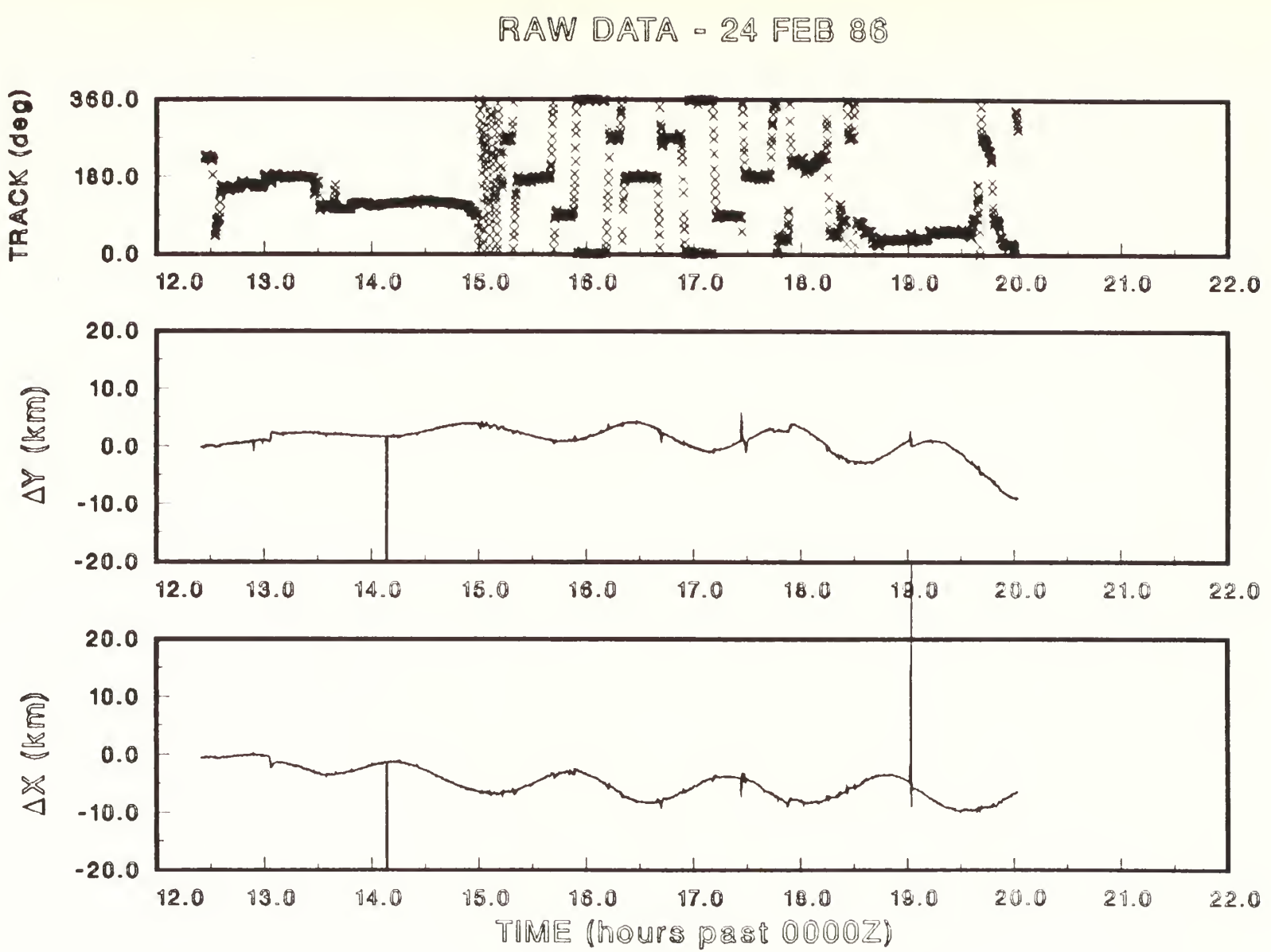
RAW DATA - 24 FEB 86
TRACK (deg)
360.0
180.0
0.0
ΔY (km)
20.0
10.0
0.0
-10.0
-20.0
ΔX (km)
20.0
10.0
0.0
-10.0
-20.0
12.0
13.0
14.0
15.0
16.0
17.0
18.0
19.0
20.0
21.0
22.0
TIME (hours past 0000Z)

B. CUBIC SPLINE FITS TO POSITION ERRORS

This appendix contains plots of the cubic spline curves fitted to the data of Appendix A. They are plotted on the same scale so that overlays can verify the fits.

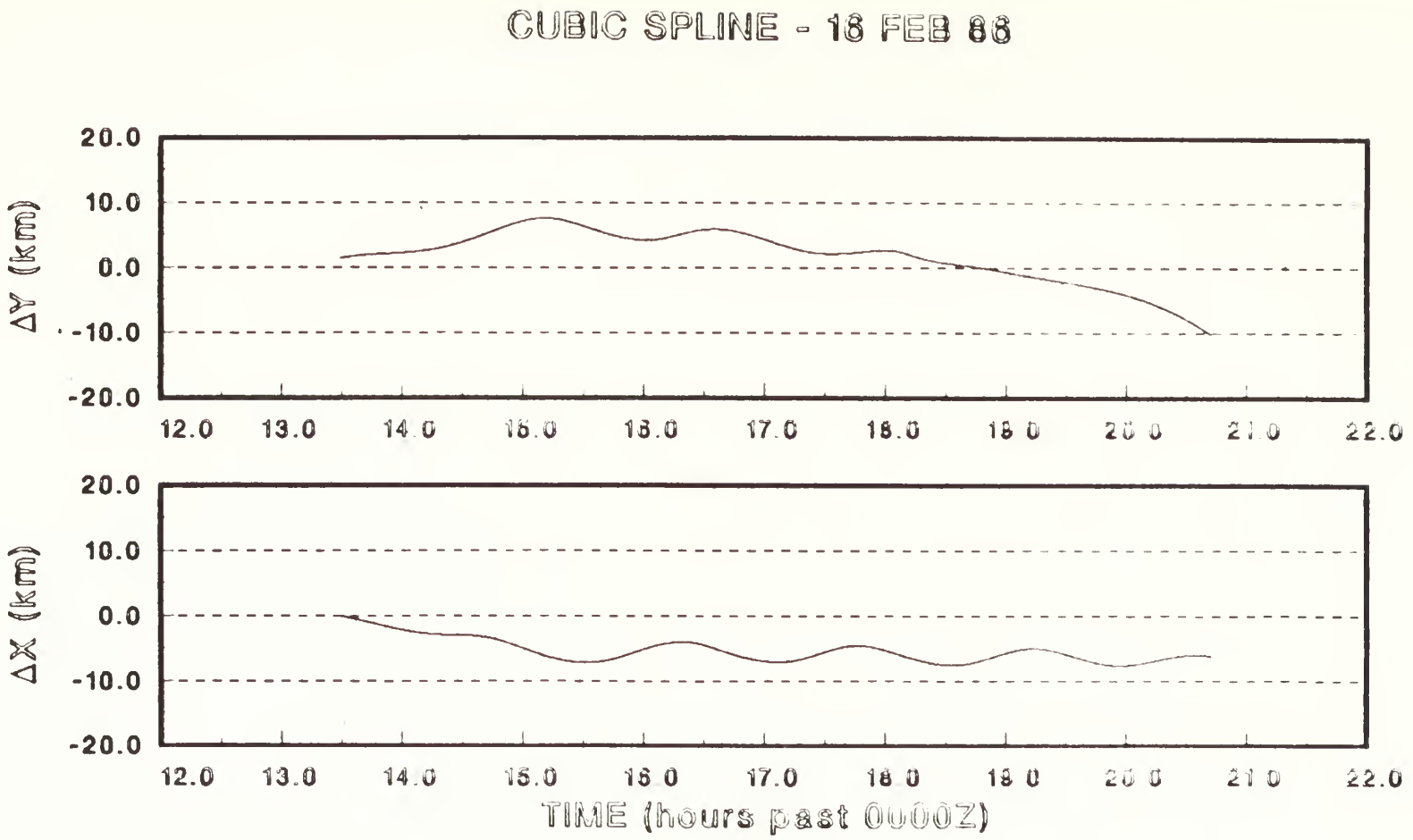
CUBIC SPLINE - 18 FEB 88
ΔY (km)
20.0
10.0
0.0
-10.0
-20.0
ΔX (km)
20.0
10.0
0.0
-10.0
-20.0
12.0
13.0
14.0
15.0
16.0
17.0
18.0
19.0
20.0
21.0
22.0
TIME (hours past 0000Z)

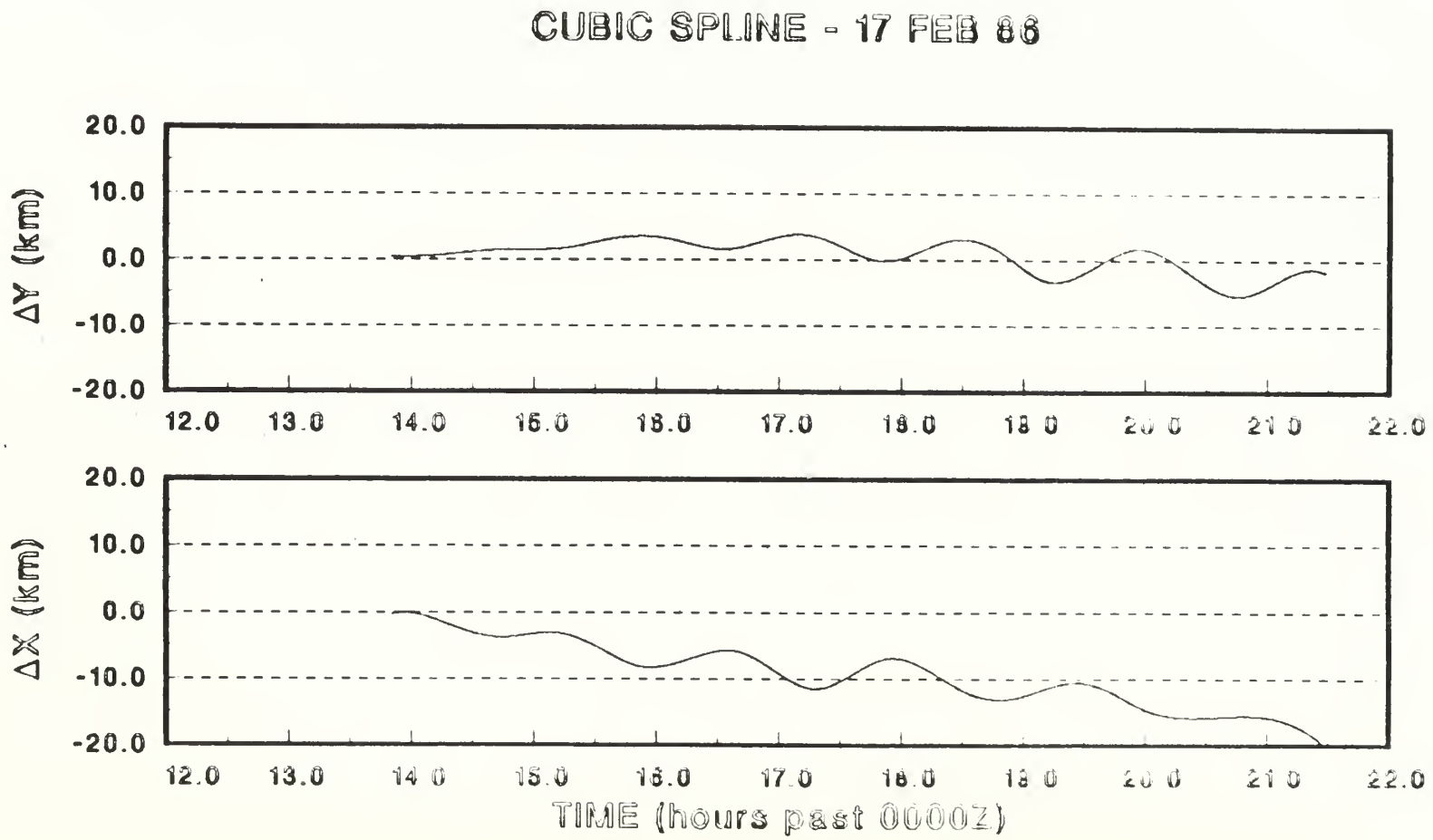
CUBIC SPLINE - 17 FEB 88
ΔY (km)
20.0
10.0
0.0
-10.0
-20.0
ΔX (km)
20.0
10.0
0.0
-10.0
-20.0
12.0
13.0
14.0
15.0
16.0
17.0
18.0
19.0
20.0
21.0
22.0
TIME (hours past 0000Z)

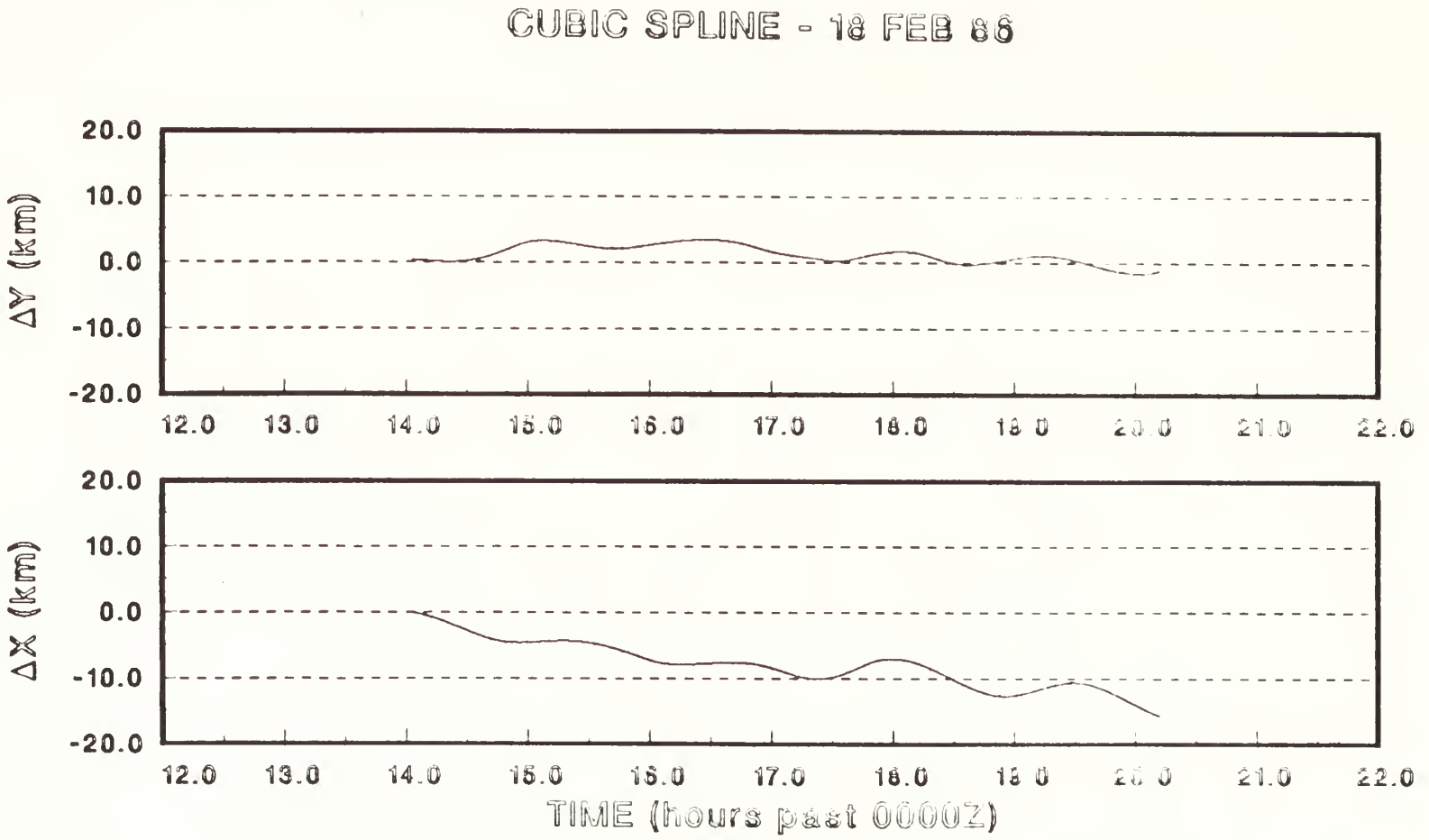
CUBIC SPLINE - 18 FEB 86
ΔY (km)
20.0
10.0
0.0
-10.0
-20.0
12.0
13.0
14.0
15.0
16.0
17.0
18.0
21.0
22.0
ΔX (km)
TIME (hours past 0000Z)

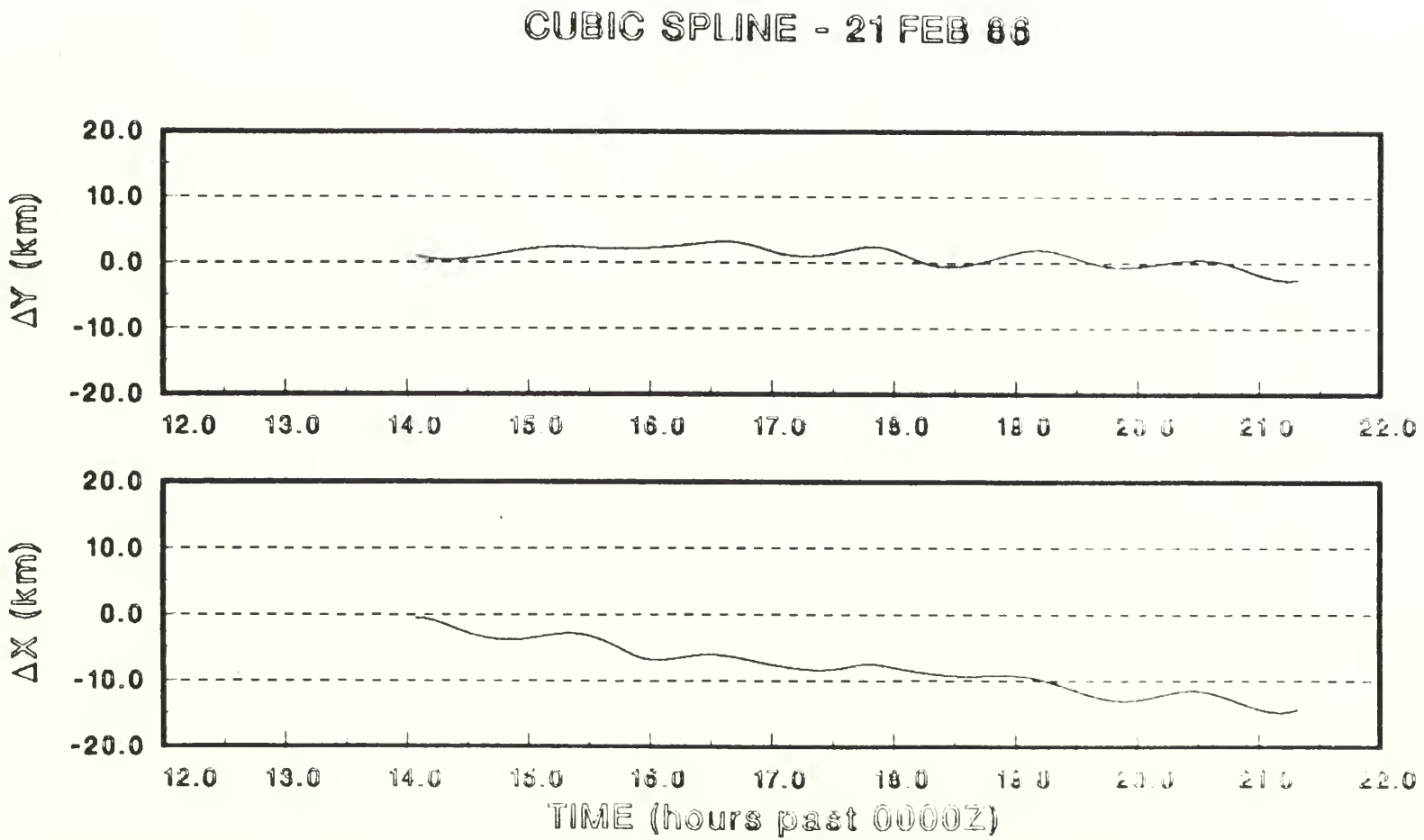
CUBIC SPLINE - 21 FEB 86
ΔY (km)
20.0
10.0
0.0
-10.0
-20.0
12.0
13.0
14.0
15.0
16.0
17.0
18.0
ΔX (km)
TIME (hours past 0000Z)

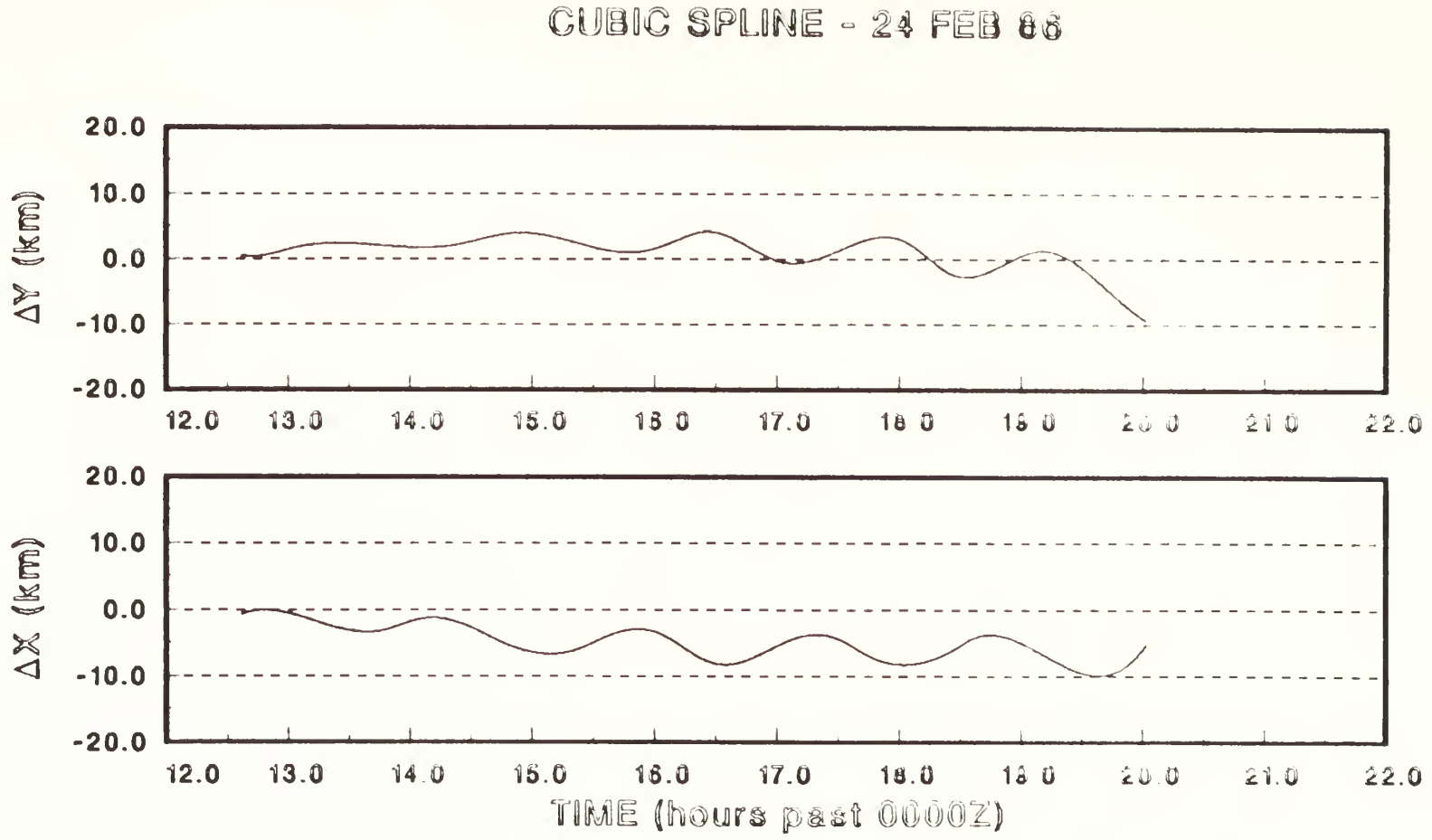
CUBIC SPLINE - 24 FEB 86
ΔY (km)
20.0
10.0
0.0
-10.0
-20.0
12.0
13.0
14.0
15.0
16.0
17.0
18.0
19.0
20.0
21.0
22.0
ΔX (km)
TIME (hours past 0000Z)

C. VELOCITY ERRORS DERIVED FROM CUBIC SPLINES

The curves which follow are the derivatives of the curves presented in Appendix B.

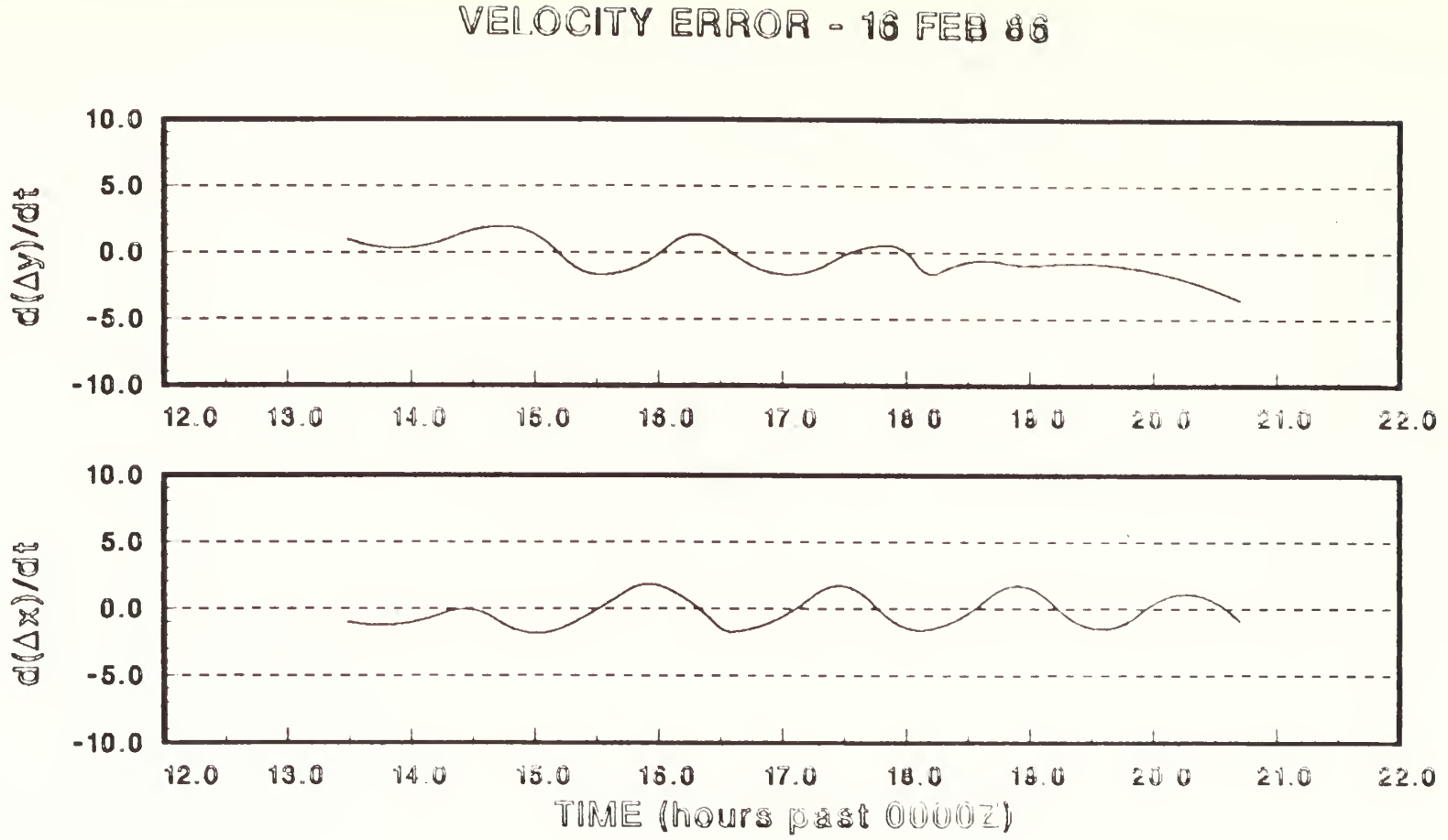
VELOCITY ERROR - 16 FEB 86
d((Δy))/dt
10.0
5.0
0.0
-5.0
-10.0
12.0
13.0
14.0
15.0
16.0
17.0
18.0
19.0
20.0
21.0
22.0
d((Δx))/dt
10.0
5.0
0.0
-5.0
-10.0
12.0
13.0
14.0
15.0
16.0
17.0
18.0
19.0
20.0
21.0
22.0
TIME (hours past 0000Z)

VELOCITY ERROR - 17 FEB 86

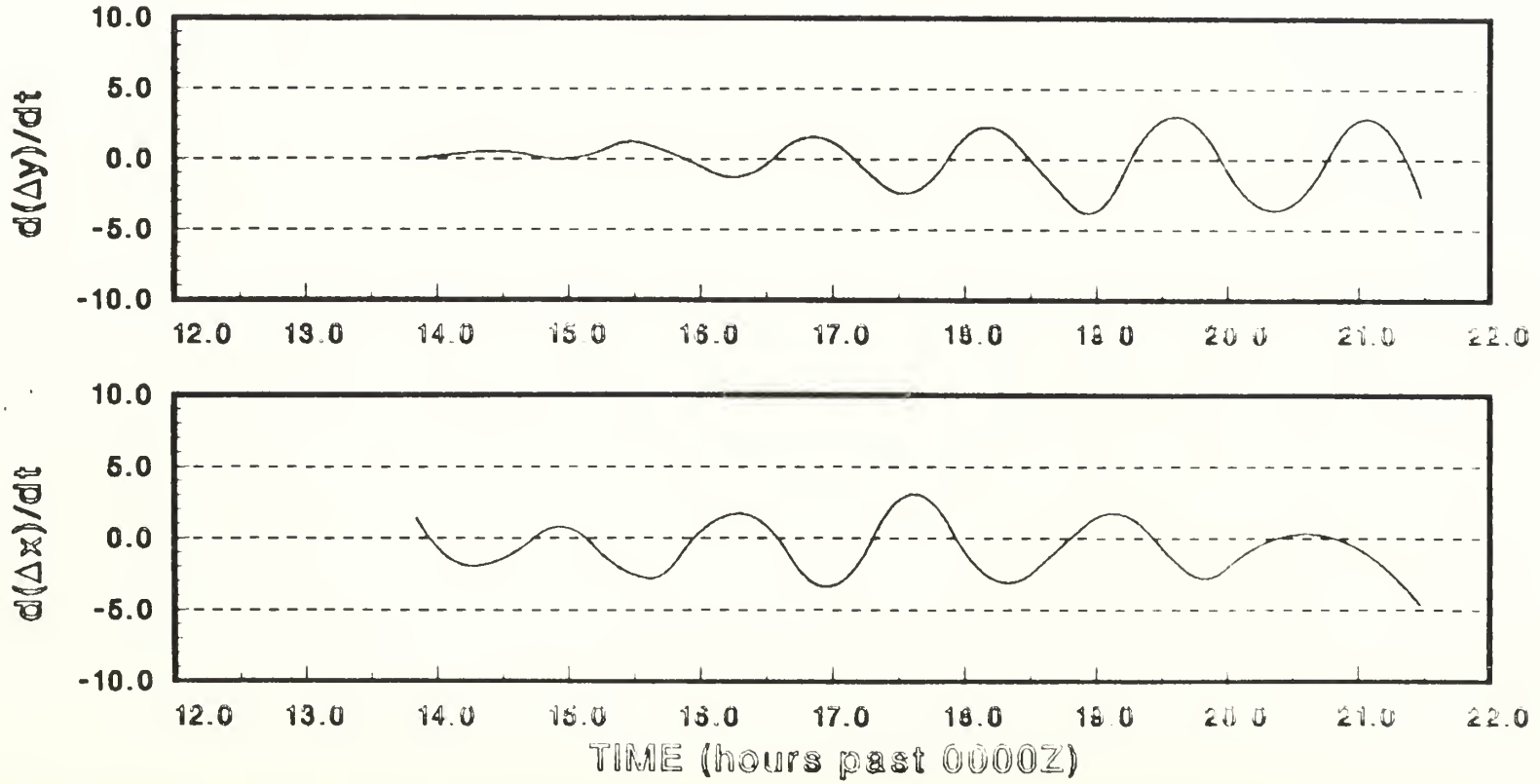

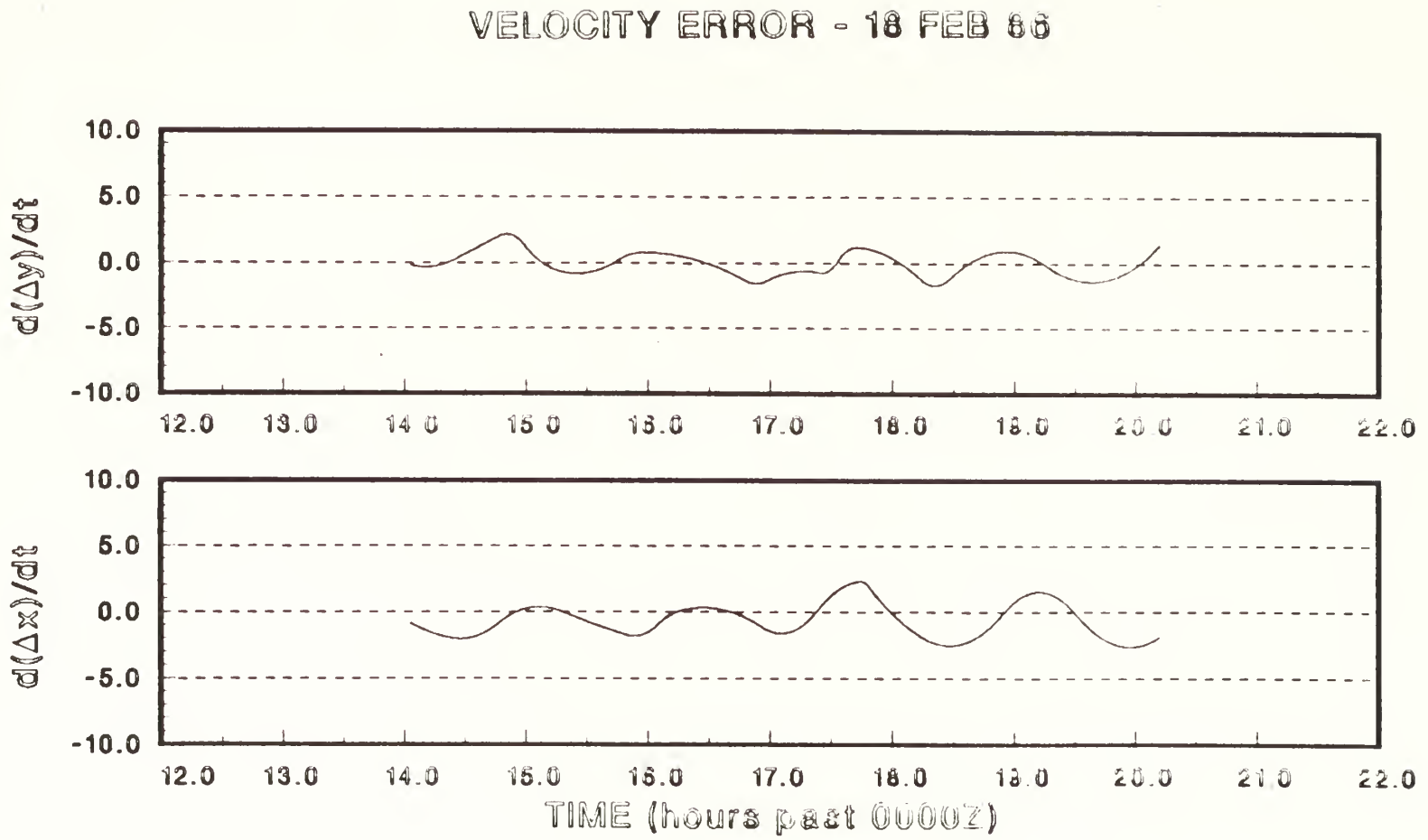
VELOCITY ERROR - 18 FEB 86
d((Δy))/dt
d((Δx))/dt
10.0
5.0
0.0
-5.0
-10.0
12.0
13.0
14.0
15.0
16.0
17.0
18.0
19.0
20.0
21.0
22.0
TIME (hours past 00000Z)

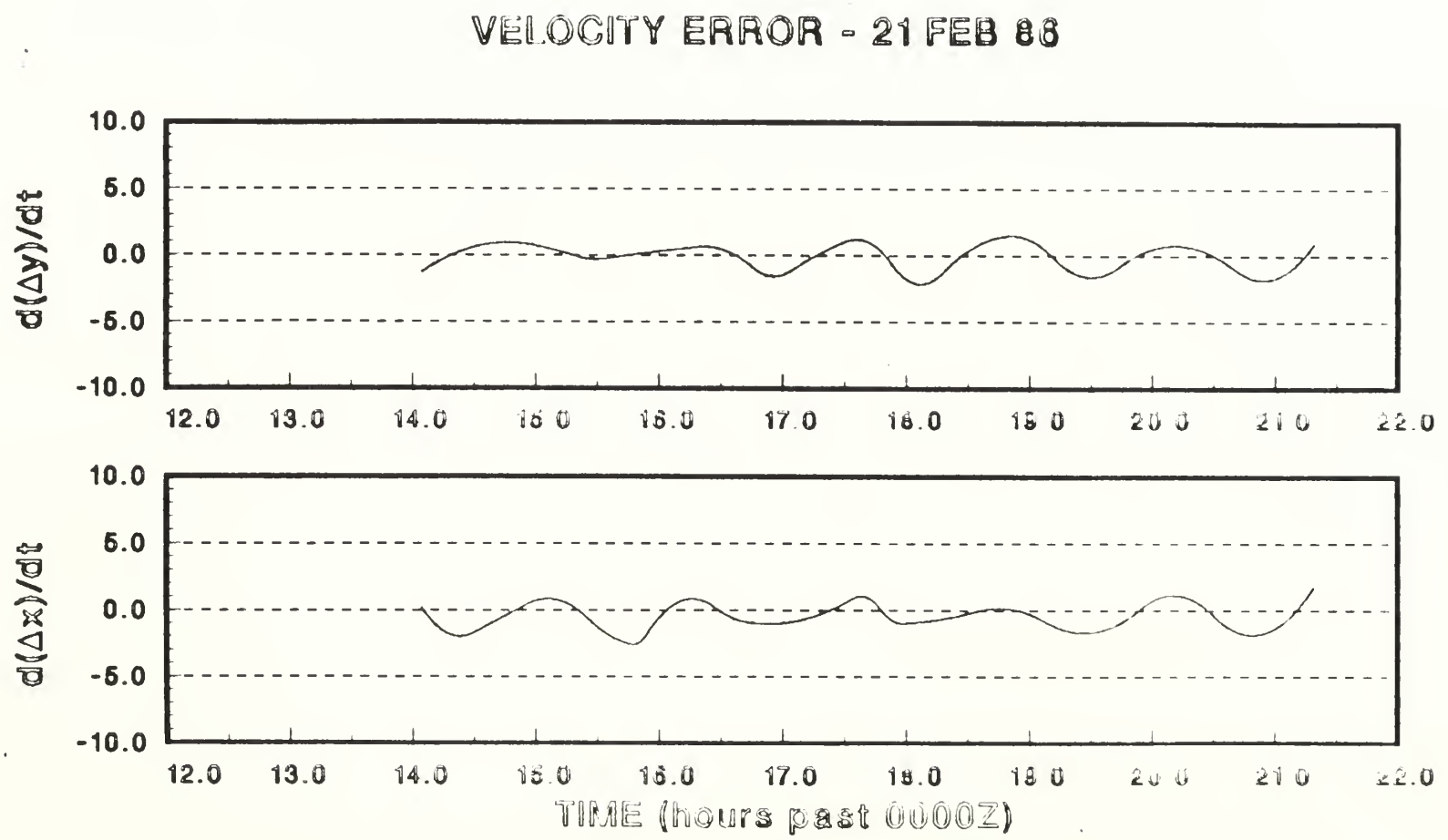
VELOCITY ERROR - 21 FEB 88
d(Δy)/dt
d(Δx)/dt
10.0
5.0
0.0
-5.0
-10.0
12.0
13.0
14.0
15.0
16.0
17.0
18.0
19.0
20.0
21.0
22.0
TIME (hours past 0000Z)

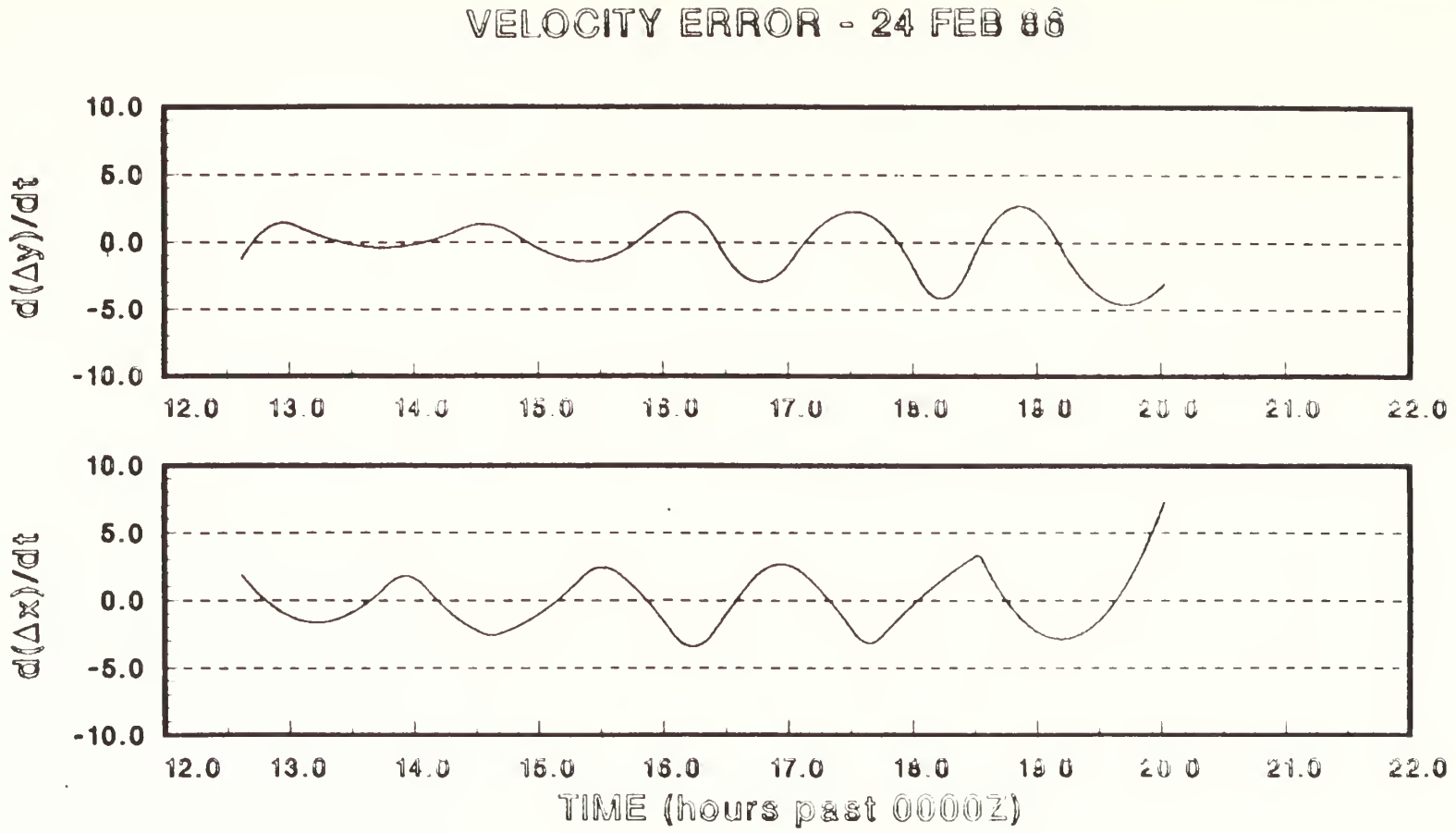
VELOCITY ERROR - 24 FEB 86
d(Δy)/dt
d(Δx)/dt
10.0
5.0
0.0
-5.0
-10.0
12.0
13.0
14.0
15.0
16.0
17.0
18.0
19.0
20.0
21.0
22.0
TIME (hours past 0000Z)

D. UNCORRECTED AND CORRECTED VELOCITY FIELDS

This section contains plots of wind vectors obtained from 100 s averages (approximately 10 km in distance) of the uncorrected and corrected wind data. Scales are identical in both cases to allow for comparison of the vector fields by overlay. Wind vectors are scaled so that 0.1 degrees of latitude or longitude is 10 m s^{-1} of windspeed. Fields are corrected only with respect to ins drifts. other potential errors, such as biases, have not been removed. also, no attempt has been made here to account for non-stationarity of wind field itself.

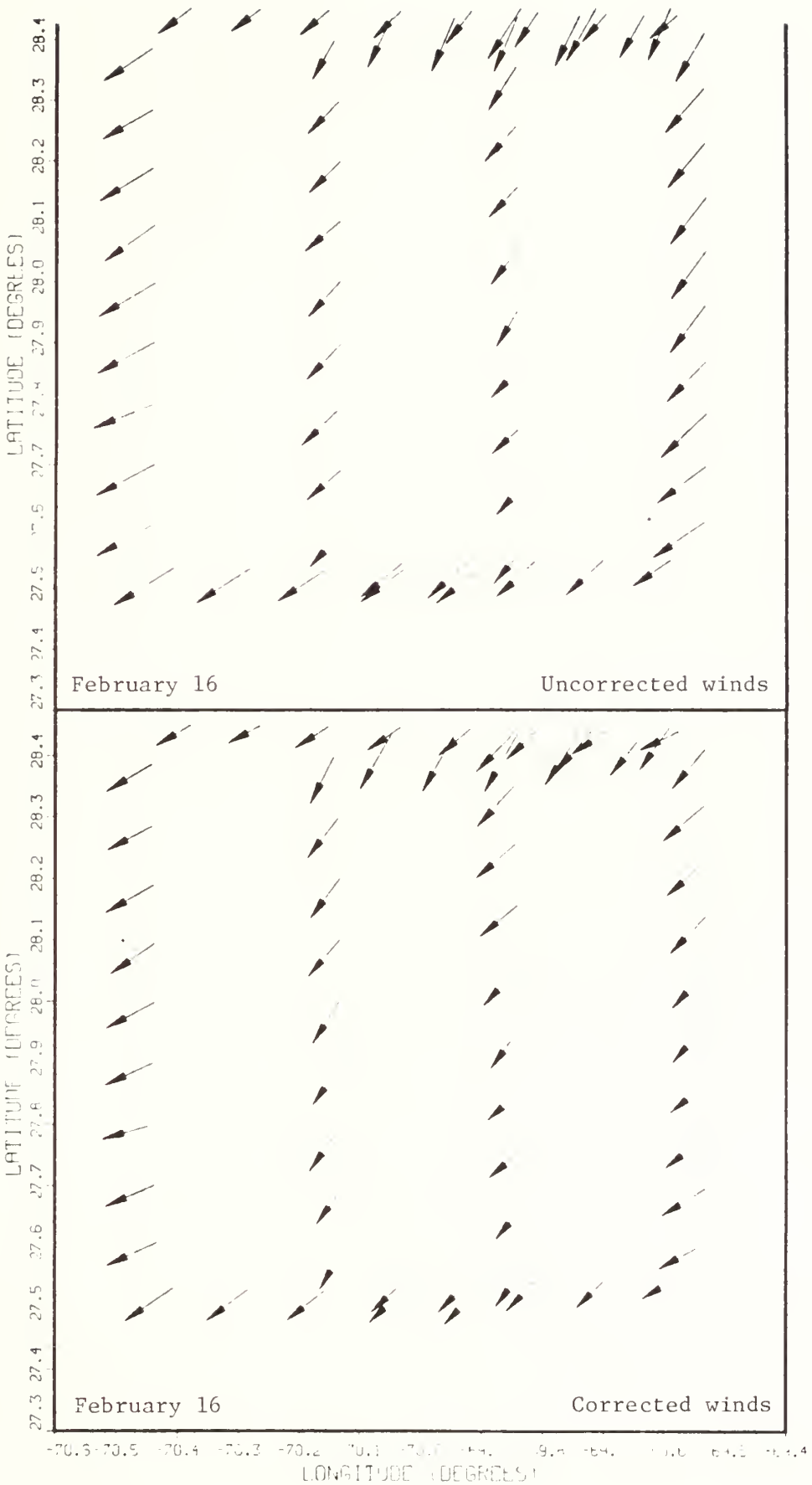
LATITUDE (DEGREES)
28.4
28.3
28.2
28.1
28.0
27.9
27.7
27.4
27.3
February 16
Uncorrected winds
February 16
Corrected winds
-70.3 -70.5 -70.4 -70.3 -70.2
LONGITUDE (DEGREES)

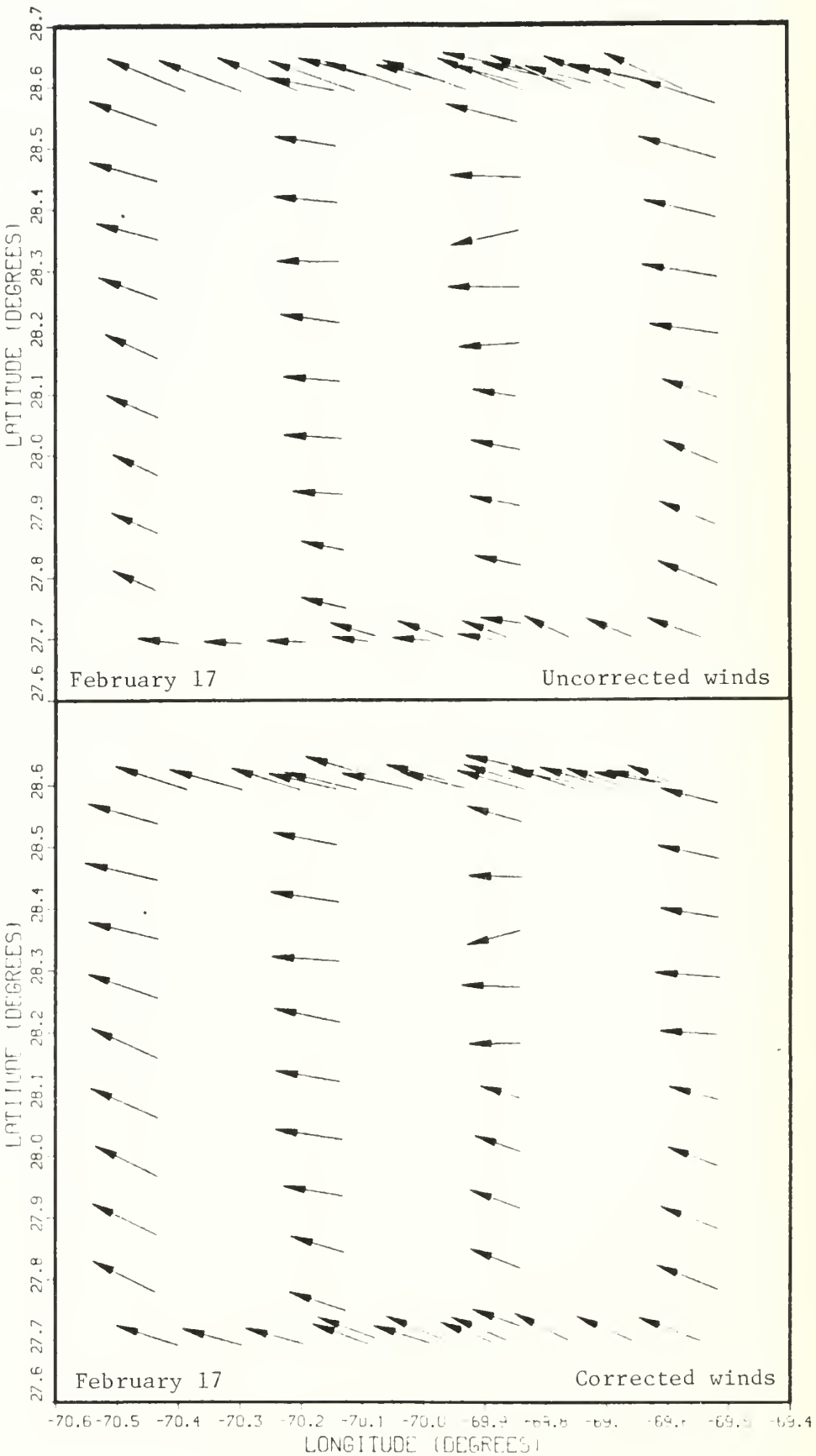
LATITUDE (DEGREES)
28.7
28.6
28.5
28.4
28.3
28.2
28.1
28.0
27.9
27.8
27.7
27.6
February 17
Uncorrected winds
LATITUDE (DEGREES)
28.6
28.5
28.4
28.3
28.2
28.1
28.0
27.9
27.8
27.7
27.6
February 17
Corrected winds
-70.6 -70.5 -70.4 -70.3 -70.2 -70.1 -70.0 -69.9 -69.8 -69. -69.4
LONGITUDE (DEGREES)

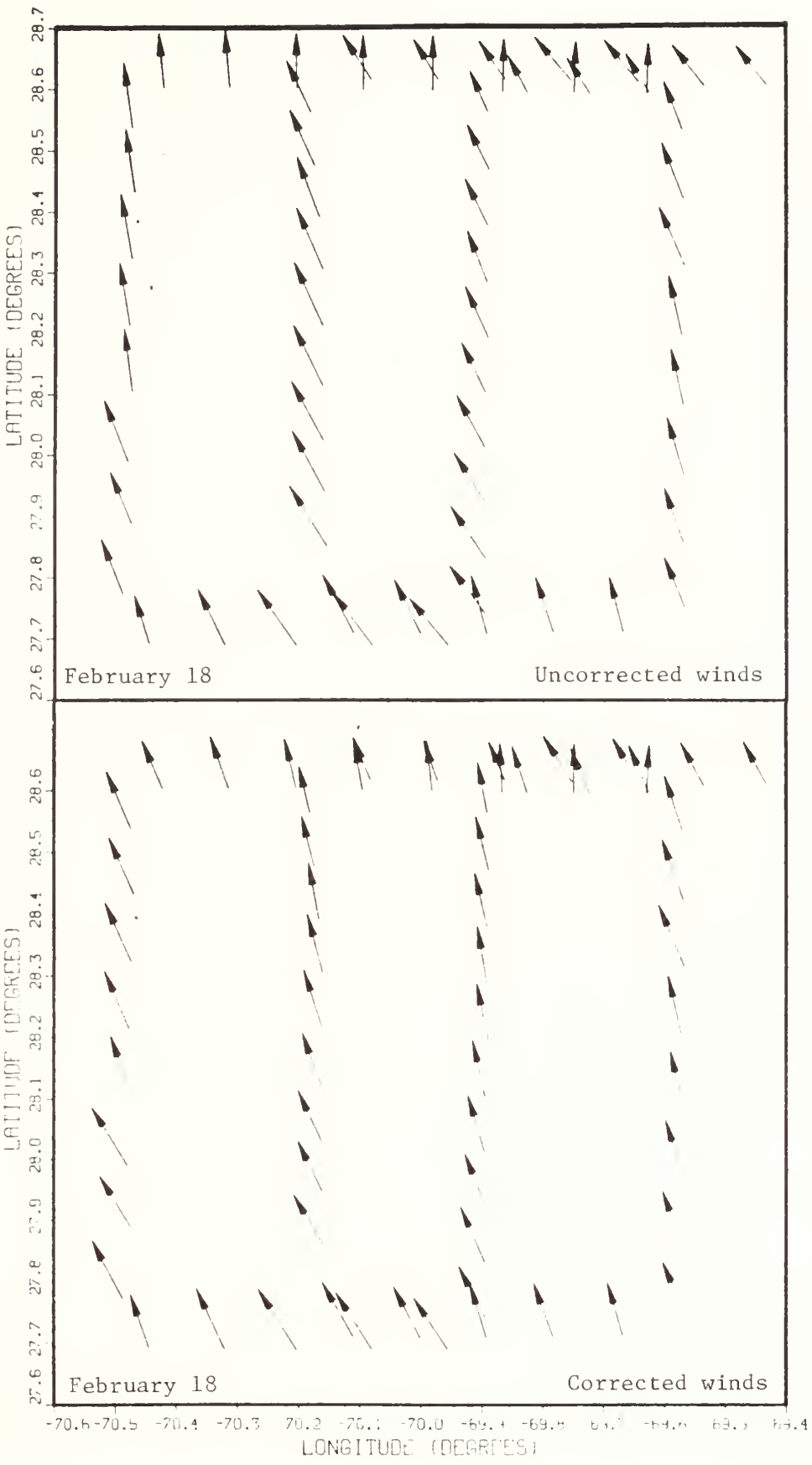
LATITUDE (DEGREES)
28.7
28.6
28.5
28.4
28.3
28.2
28.1
28.0
27.9
27.8
27.7
27.6
February 18
Uncorrected winds
LATITUDE (DEGREES)
28.6
28.5
28.4
28.3
28.2
28.1
28.0
27.9
27.8
27.7
27.6
February 18
Corrected winds
-70.6 -70.5 -70.4 -70.3 -70.2 -70.1 -70.0 -69.9 -69.8 -69.7 -69.6 -69.5 -69.4
LONGITUDE (DEGREES)

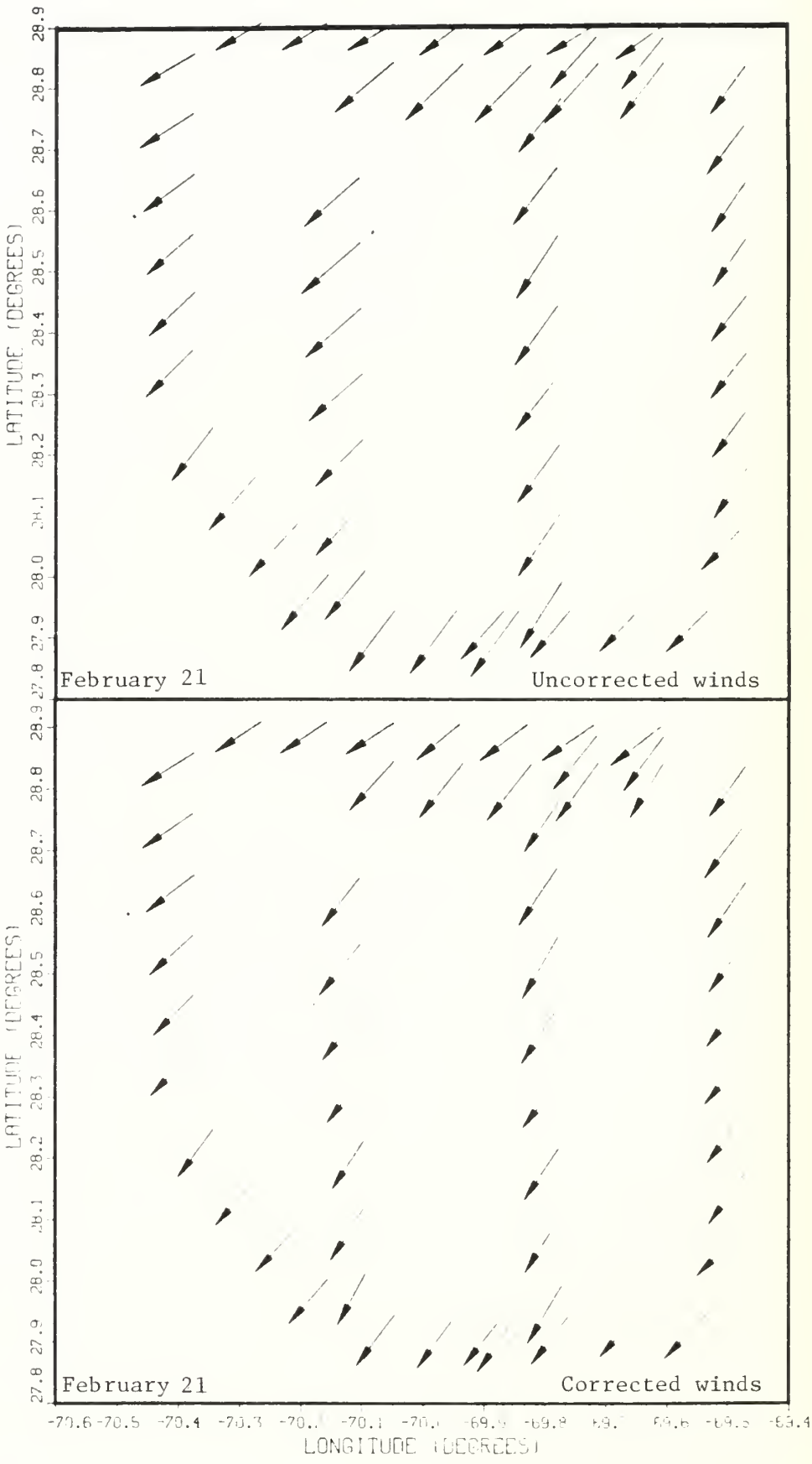
LATITUDE (DEGREES)
28.9
28.8
28.7
28.6
28.5
28.4
28.3
28.2
28.1
28.0
27.9
27.8
February 21
Uncorrected winds
February 21
Corrected winds
-70.6 -70.5 -70.4 -70.3
LONGITUDE (DEGREES)

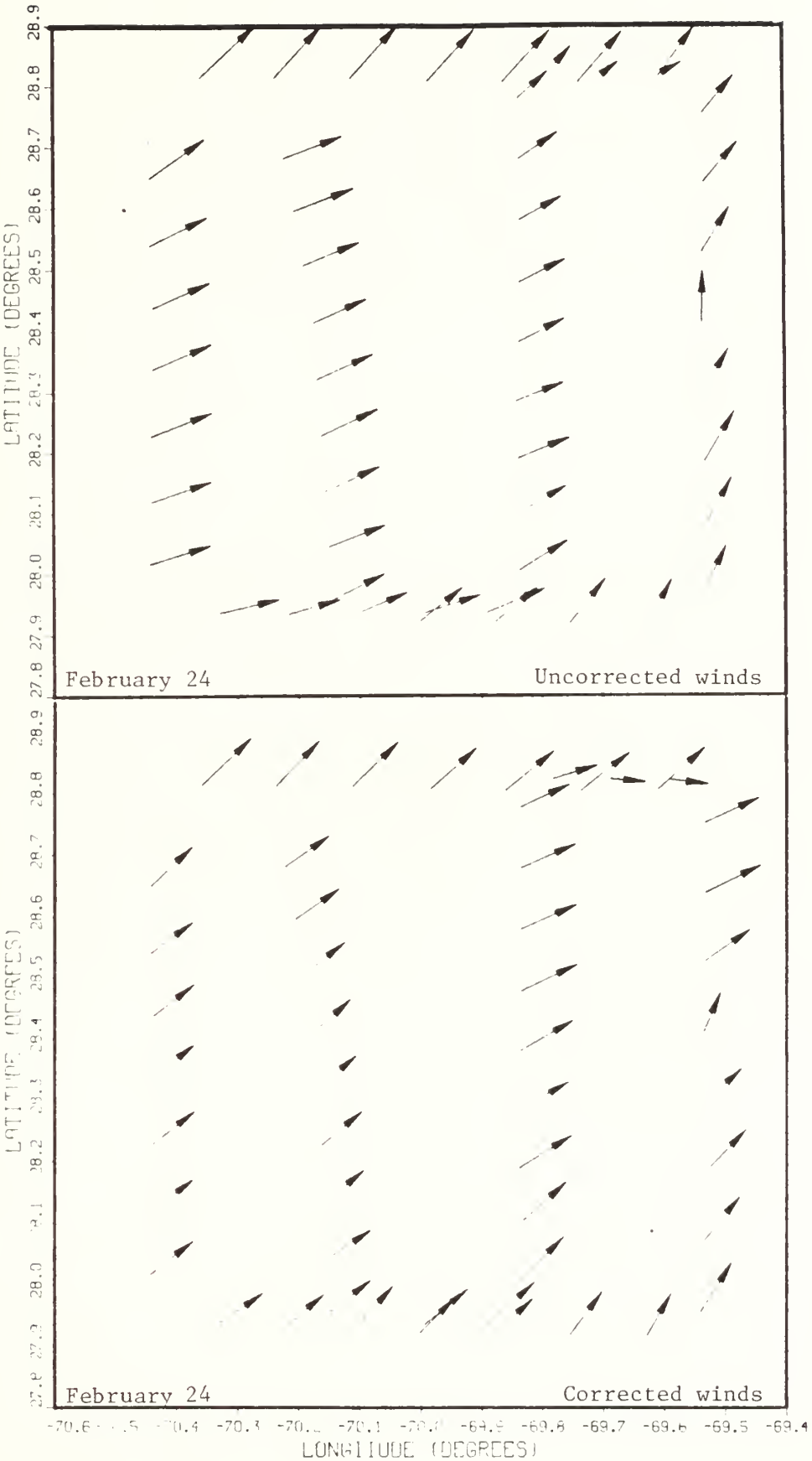
LATITUDE (DEGREES)
28.9
28.8
28.7
28.6
28.5
28.4
28.3
28.2
28.1
28.0
27.9
27.8
February 24
Uncorrected winds
LATITUDE (DEGREES)
28.9
28.8
28.7
28.6
28.5
28.4
28.3
28.2
28.1
28.0
27.9
27.8
February 24
Corrected winds
-70.6
-70.5
-70.4
-70.3
-70.2
-70.1
-70.0
-69.9
-69.8
-69.7
-69.6
-69.5
-69.4
LONGITUDE (DEGREES)

E. SETS OF SPLINE COEFFICIENTS

Following are the sets of spline coefficients for the correction of INS-derived position and horizontal wind velocity components in an east-north coordinate system. These coefficients have been determined for the five (out of six) correctable Electra flights in FASINEX. With the coefficients supplied, the output is in km for position error and in $m\ s^{-1}$ for the velocity errors.

E.1 Spline Evaluation Subroutine

```
      SUBROUTINE SPLINE(XK,C,CINT,N,T,VAL,DER)
C
C   SUBROUTINE TO EVALUATE THE A CUBIC SPLINE AND ITS FIRST
C   DERIVATIVE AT A PARTICULAR ABSCISSA VALUE T
C
C     XK --    INPUT     ARRAY OF N KNOTS FOR THE N SPLINES
C                        SENT TO THIS ROUTINE
C     C --     INPUT     ARRAY OF (3,N) CUBIC SPLINE
C                        COEFFICIENTS
C     CINT --  INPUT     ARRAY OF N SPLINE INTERCEPT VALUES
C     N --     INPUT     NUMBER SETS OF CUBIC SPLINE
C                        COEFFICIENTS IN FUNC
C     T --     INPUT     ABSCISSA (E.G. TIME) VALUE AT WHICH
C                        THE CUBIC SPLINE FUNCTION AND ITS
C                        FIRST DERIVATIVE ARE TO BE
C                        EVALUATED (IN SECS)
C     VAL --   OUTPUT    VALUE OF SPLINE AT TIME T (IN KM)
C     DER --   OUTPUT    VALUE OF FIRST DERIVATIVE AT TIME T
C                        (IN M/SEC)
C
      DIMENSION XK(1),C(3,N),CINT(1)
C
      DO 10 I=1,N
      IF(XK(I).GT.T) GO TO 20
   10 CONTINUE
C
   20 IF(I.GT.1) GO TO 30
      VAL = -9999.
      DER = -9999.
      RETURN
C
   30 I = I-1
      D =(T - XK(I)) / 1000
      VAL = CINT(N) + D*(C(1,N) + D*(C(2,N) + D*C(3,N)))
      DER = D*(2*C(2,N) + D*3*C(3,N)) + C(1,N)
      RETURN
      END
```

E.2 Spline Coefficients

February 16 - DELTA X COEF:

XK (SECS PAST 0000Z)	CINT	C(1,N)	C(2,N)	C(3,N)
48535	0.005	-0.996	-0.256	0.087
50065	-1.804	-1.165	0.145	0.088
51360	-2.878	-0.345	0.488	-0.288
52889	-3.297	-0.877	-0.835	0.238
54966	-6.592	-1.273	0.644	0.040
56638	-6.731	1.219	0.846	-0.414
57714	-4.957	1.603	-0.489	-0.177
59242	-4.284	-1.138	-1.303	0.920
59750	-5.075	-1.749	0.096	0.135
62074	-6.919	0.895	1.041	-0.455
63858	-4.590	0.270	-1.391	0.342
65393	-6.218	-1.585	0.183	0.175
67162	-7.482	0.703	1.111	-0.424
69063	-5.044	0.328	-1.308	0.307
71634	-7.633	-0.317	1.057	-0.269

February 16 - DELTA Y COEF:

XK (SECS PAST 0000Z)	CINT	C(1,N)	C(2,N)	C(3,N)
48535	1.381	0.909	-0.436	0.105
50270	2.193	0.342	0.108	0.083
52003	3.541	1.463	0.539	-0.192
53736	6.697	1.602	-0.459	-0.273
54852	7.534	-0.441	-1.372	0.484
55902	6.117	-1.721	0.155	0.115
58442	4.625	1.286	1.029	-1.095
59141	5.652	1.122	-1.264	0.192
62533	2.406	-0.825	0.690	-0.106
64180	2.446	0.586	0.167	-1.168
64602	2.635	0.103	-1.312	0.447
65673	1.789	-1.170	0.124	-0.013
69973	-2.000	-0.839	-0.047	-0.035

February 17 - DELTA X COEF:

XK (SECS PAST 0000Z)	CINT	C(1,N)	C(2,N)	C(3,N)
49800	-0.347	1.479	-2.212	0.474
51419	-1.737	-1.957	0.088	0.209
53037	-3.790	-0.034	1.101	-0.511
54656	-3.130	-0.488	-1.381	0.270
56145	-6.029	-2.807	-0.175	0.804
56981	-8.028	-1.415	1.841	-0.365
58673	-6.918	1.681	-0.013	-0.530
60014	-5.965	-1.213	-2.145	0.706
62294	-11.506	0.024	2.687	-0.797
64429	-6.964	0.600	-2.417	0.521
66725	-12.026	-2.265	1.169	-0.006
68046	-12.990	0.795	1.147	-0.472
69936	-10.576	0.070	-1.530	0.176
70839	-11.630	-2.262	-1.053	0.655
71944	-14.531	-2.191	1.117	-0.168

February 17 - DELTA Y COEF:

XK (SECS PAST 0000Z)	CINT	C(1,N)	C(2,N)	C(3,N)
49800	0.322	-0.028	0.158	-0.003
51419	0.677	0.457	0.141	-0.091
53037	1.399	0.197	-0.302	0.145
55151	1.837	0.867	0.619	-0.374
56065	2.861	1.061	-0.406	-0.048
57884	3.159	-0.892	-0.668	0.368
59671	1.531	0.245	1.304	-0.436
61641	3.742	0.306	-1.274	0.065
62514	3.082	-1.768	-1.103	0.588
64320	-0.247	0.001	2.082	-0.639
66166	2.832	1.160	-1.455	0.014
67705	1.224	-3.217	-1.390	1.015
69102	-3.219	-1.158	2.864	-0.653
71819	1.676	-0.060	-2.460	0.564
74787	-5.431	0.234	2.559	-0.828

February 18 - DELTA X COEF:

XK (SECS PAST 0000Z)	CINT	C(1,N)	C(2,N)	C(3,N)
50582	-0.125	-0.869	-0.735	0.146
51884	-2.182	-2.041	-0.165	0.309
53188	-4.438	-0.900	1.041	-0.293
54490	-4.493	0.319	-0.105	-0.215
55154	-4.391	-0.105	-0.533	0.028
56988	-6.206	-1.781	-0.381	0.605
57876	-7.664	-1.028	1.229	-0.426
58591	-7.926	0.077	0.315	-0.162
60973	-8.143	-1.178	-0.842	0.506
62600	-10.108	0.098	1.627	-0.399
63843	-8.240	2.290	0.136	-2.161
64121	-7.638	1.864	-1.670	0.196
65781	-8.245	-2.055	-0.692	0.324
68059	-12.690	-0.161	1.523	-0.469
70229	-10.666	-0.178	-1.531	0.318

February 18 - DELTA Y COEF:

XK (SECS PAST 0000Z)	CINT	C(1,N)	C(2,N)	C(3,N)
50582	0.274	-0.209	-0.342	0.262
51884	0.002	0.235	0.682	-0.004
53188	1.454	1.989	0.665	-0.973
53968	2.950	1.246	-1.615	0.456
54796	3.134	-0.490	-0.485	0.229
56723	2.028	0.195	0.840	-0.410
57391	2.412	0.769	0.019	-0.079
60488	2.641	-1.374	-0.711	0.792
61072	1.754	-1.394	0.676	-0.199
62654	0.453	-0.748	-0.268	1.406
63182	0.190	0.140	1.955	-1.201
63748	0.678	1.198	-0.088	-0.199
65604	1.329	-1.182	-1.195	0.917
66492	-0.022	-1.136	1.248	-0.252
69352	1.033	-0.189	-0.917	0.230

February 21 - DELTA X COEF:

XK (SECS PAST 0000Z)	CINT	C(1,N)	C(2,N)	C(3,N)
50652	-0.584	0.227	-1.965	0.577
52188	-2.775	-1.724	0.693	-0.003
53722	-3.797	0.387	0.682	-0.360
55513	-2.983	-0.631	-1.250	0.250
56791	-5.311	-2.601	-0.291	1.685
57244	-6.391	-1.830	1.996	-0.501
59223	-6.076	0.188	-0.976	0.271
60205	-6.577	-0.946	-0.178	0.105
63227	-8.175	0.845	0.770	-1.014
64044	-7.524	0.078	-1.710	0.895
64707	-7.964	-1.009	0.073	0.044
66845	-9.358	-0.097	0.353	-0.180
68873	-9.604	-0.887	-0.743	0.220
71639	-13.081	0.058	1.084	-0.368
73796	-11.610	-0.404	-1.298	0.379

February 21 - DELTA Y COEF:

XK (SECS PAST 0000Z)	CINT	C(1,N)	C(2,N)	C(3,N)
50652	0.914	-1.338	0.883	-0.116
52188	0.521	0.553	0.349	-0.116
53873	1.888	0.740	-0.237	-0.038
55257	2.357	-0.136	-0.396	0.262
56005	2.143	-0.288	0.193	-0.008
58727	2.639	0.596	0.132	-0.252
60339	2.887	-0.942	-1.086	0.596
61421	1.352	-1.197	0.850	-0.067
63037	1.355	1.026	0.525	-0.576
64378	2.288	-0.668	-1.789	0.710
65845	-0.302	-1.333	1.336	-0.210
67731	0.527	1.463	0.146	-0.362
69089	1.875	-0.145	-1.331	0.397
71018	-0.505	-0.845	0.968	-0.196
74402	0.144	-1.011	-1.017	0.409

February 24 - DELTA X COEF:

XK (SECS PAST 0000Z)	CINT	C(1,N)	C(2,N)	C(3,N)
45404	-0.714	1.912	-1.624	0.248
46809	-0.549	-1.186	-0.579	0.247
48216	-2.673	-1.347	0.464	0.191
49621	-3.117	1.094	1.272	-0.806
50768	-1.406	0.832	-1.500	0.203
52434	-3.243	-2.473	-0.484	0.770
52815	-4.213	-2.506	0.397	0.125
55223	-6.203	1.578	1.300	-0.687
56360	-3.734	1.869	-1.045	-0.171
57839	-3.806	-2.340	-1.804	0.990
59085	-7.610	-2.220	1.899	-0.089
59977	-8.143	0.954	1.660	-0.548
61703	-4.369	1.791	-1.175	-0.158
63074	-4.531	-2.326	-1.826	1.326
63882	-6.905	-2.678	1.391	-0.076
66634	-5.317	3.259	0.767	-6.039
66817	-4.732	2.933	-2.549	0.373

February 24 - DELTA Y COEF:

XK (SECS PAST 0000Z)	CINT	C(1,N)	C(2,N)	C(3,N)
45404	0.539	-1.279	2.188	-0.591
46975	1.637	1.216	-0.600	0.069
48546	2.333	-0.159	-0.275	0.097
49718	1.925	-0.403	0.067	0.085
51751	2.100	0.926	0.587	-0.298
53382	3.878	0.464	-0.870	0.122
54768	3.177	-1.243	-0.362	0.213
57005	0.968	0.336	1.066	-0.082
57837	1.937	1.938	0.860	-0.796
59184	4.162	-0.082	-2.359	0.649
61384	-0.530	-1.043	1.923	-0.373
63128	1.522	2.263	-0.026	-0.471
64927	2.770	-2.397	-2.565	1.218
66457	-2.541	-1.682	3.031	-0.701
69029	1.255	-0.003	-2.378	0.407

F. DIVERGENCE ERROR FROM THE SCHULER OSCILLATION

It is useful to consider what error an 84.4-min sinusoidal oscillation may induce in a line integral calculation of the horizontal divergence. The divergence is expressed as

$$\vec{\nabla} \cdot \vec{V}_H = \frac{1}{A} \int (\vec{V}_H \cdot \vec{n})\, dl \qquad (F.1)$$

where $\vec{V}_H$ is the horizontal wind vector, $\vec{n}$ is a unit vector normal to the flight track, and dl is an increment of distance along the track.

For simplicity, we restrict our flight geometry to a square box with a perimeter of length C which is flown counterclockwise at a constant groundspeed S beginning at the southeastern corner. We further assume that the box sides are oriented east-west and north-south and that the earth's curvature may be neglected. Considering only the error in the east component of velocity, we may represent the oscillation as

$$U_\epsilon = a \sin\left(\frac{2\pi t}{T} + \phi\right) \qquad (F.2)$$

where a is the amplitude, T is 84.4 min, and ϕ is an arbitrary phase. Noting that contributions to the integral from the east component of the error come only from the north-south legs and that dl = S dt, we may write

$$\epsilon_U = \vec{\nabla} \cdot \vec{U}_\epsilon = \frac{1}{A} \int_0^{C/4S} U_\epsilon\, S\, dt - \frac{1}{A} \int_{3C/4S}^{C/S} U_\epsilon\, S\, dt \qquad (F.3)$$

$$= aS \cdot \frac{-T}{2\pi A} \left[\cos\left(\frac{2\pi t}{T} + \phi\right) \Big|_0^{C/4S} - \cos\left(\frac{2\pi t}{T} + \phi\right) \Big|_{3C/4S}^{C/S} \right]$$

$$= \frac{aST}{2\pi A} \left[\cos(B+\phi) - \cos(3B/4+\phi) - \cos(B/4+\phi) + \cos\phi \right]$$

where $B = 2\pi C/ST$.

Since the error depends on the random phase ϕ at the beginning of the box, we determine the maximum divergence error by maximizing the error with respect to ϕ as follows. (F.3) may be rewritten

$$\epsilon_U = \frac{aST}{2\pi A} \left[\cos B\cos\phi - \sin B\sin\phi - \cos(3B/4)\cos\phi + \sin(3B/4)\sin\phi - \cos(B/4)\cos\phi + \sin(B/4)\sin\phi + \cos\phi \right] \quad \text{(F.4)}$$

To maximize the error,

$$0 = \frac{\partial \epsilon_U}{\partial \phi} = \frac{aST}{2\pi A} \left[-\cos B\sin\phi - \sin B\cos\phi + \cos(3B/4)\sin\phi + \sin(3B/4)\cos\phi + \cos(B/4)\sin\phi + \sin(B/4)\cos\phi - \sin\phi \right] \quad \text{(F.5)}$$

This is true if the argument in square brackets is zero. A little rearranging yields

$$\tan\phi = \frac{\left[\sin(-B) + \sin(3B/4) + \sin(B/4) \right]}{\left[\cos B - \cos(3B/4) - \cos(B/4) + 1 \right]} \quad \text{(F.6)}$$

For $C = 400$ km, $S = 100$ m s^{-1}, and $T = 84.4$ min,

$$\phi = 0.66 \text{ rad (or } 37.82°)$$

Substituting these values into F.4 yields

$$\epsilon_U = 5.4 \times 10^{-5} \text{ s}^{-1}$$

This error is additive with the contribution to the divergence from the error in the north component of velocity. Therefore, the error in the divergence could be as large as 10^{-4} s^{-1}. The position difference data quality appears high enough to expect an effective reduction of at least an order of magnitude in the Schuler amplitude a. As a result, the error in divergence due to the INS drifts after correction should be no more than 10^{-5} s^{-1}.

Distribution List

	No. of Copies
Dr. Robert F. Abbey Office of Naval Research 800 N. Quincy Street Arlington, VA 22217	1
Dr. Joost Businger NCAR P. O. Box 3000 Boulder, CO 80307	1
Dr. Kenneth Davidson Department of Meteorology Code 63Ds Naval Postgraduate School Monterey, CA 93943-5000	1
Dr. Carl Friehe Mechanical Engineering University of California, Irvine Irvine, CA 92717	2
Dr. Gary K. Greenhut NOAA/ERL R/E2 325 Broadway Boulder, CO 80303	1
Dr. Howard Hanson CIRES P. O. Box 449 Boulder, CO 80309	1
Dr. Warren Johnson NCAR P. O. Box 3000 Boulder, CO 80307	1
Dr. Siri Jodha Singh Khalsa CIRES P. O. Box 449 Boulder, CO 80309	1
Dr. Bill Large NCAR P. O. Box 3000 Boulder, CO 80307	1
Dr. Don Lenschow NCAR P. O. Box 3000 Boulder, CO 80307	1

Dr. F. K. Li 1
Jet Propulsion Laboratory
MS 183-701
4800 Oak Grove Drive
Pasadena, CA 91109

Dr. William Plant 1
Code 7913S
Naval Research Laboratory
Washington, DC 20375

Dr. Robert J. Renard, Chairman 1
Department of Meteorology, Code 63Rd
Naval Postgraduate School
Monterey, CA 93943-5000

Dr. William J. Shaw 12
Department of Meteorology, Code 63Sr
Naval Postgraduate School
Monterey, CA 93943-5000

Dr. Steve Stage 2
Department of Meteorology
Florida State University
Tallahassee, FL 32301

Dr. Robert A. Weller 1
Woods Hole Oceanographic Institution
Woods Hole, MA 02543

Library, Code 0142 2
Naval Postgraduate School
Monterey, CA 93943-5000

Research Administration, Code 012 1
Naval Postgraduate School
Monterey, CA 93943-5000

Defense Technical Information Center 2
Cameron Station
Alexandria, VA 22304-6145

National Science Foundation 1
Washington, DC 20550